# MODELLING IMPACT BASIN IN ANSYS FLUENT AND EVALUATE ITS PERFORMANCE

A Dissertation submitted in partial fulfilment of the requirement for the
Award of degree of

**MASTER OF TECHNOLOGY**

**IN**

**HYDRAULICS AND WATER RESOURCES ENGINEERING**

**BY**

ISHAN SHARMA
(2K15/HFE/09)

**Under The Guidance of**

**RAKESH MEHROTRA**

**Associate Professor**
**Department of Civil Engineering**
**Delhi Technological University**
**Delhi**

**DELHI TECHNOLOGICAL UNIVERSITY**

**(FORMELY DELHI COLLEGE OF ENGINEERING)**

**DELHI-110042**

**JULY 2017**

# CANDIDATES'S DECLARATION

I do hereby certify that the work presented is the report entitled **"Modelling Impact Basin in Ansys Fluent and evaluate its performance** " in the partial fulfilment of the requirements for the award of the degree of "Master of Technology" in Hydraulics & Water Resources Engineering submitted in the Department of Civil Engineering, Delhi Technological University, is an authentic record of my own work carried out from January 2017 to July 2017 under the supervision of Rakesh Mehrotra (Associate Professor), Department of Civil engineering.

I have not submitted the matter embodied in the report for the award of any other degree or diploma.

Date: 30/06/2017

Ishan Sharma
2K15/HFE/09

---

## CERTIFICATE

This is to certify that above statement made by the candidate is correct to best of my knowledge.

Rakesh Mehrotra
(Associate Professor)
Department of Civil Engineering
Delhi Technological University

# ACKNOWLEDGEMENT

I take this opportunity to express my profound gratitude and deep regards to Rakesh Mehrotra (Associate Professor, Civil Engineering Department, DTU) for his exemplary guidance, monitoring and constant encouragement throughout the course for this project work. The blessing, help and guidance given by him from time to time shall carry me a long way in life on which I am going to embark.

I would also like to thank Dr. Nirendra Dev (Head of Department, Civil Engineering Department, DTU) for extending his support and Guidance.

Professors and faculties of the department of Civil Engineering, DTU, have always extended their full co-operation and help. They have been kind enough to give their opinions on the project matter; I am deeply obliged to them. They have been a source of encouragement and have continuously been supporting me with their knowledge base, during study. Several of well wishers extended their help to me directly or indirectly and we grateful to all of them without whom it would have been impossible for me to carry on my work.

# ABSTRACT

In this Dissertation computational fluid dynamics (CFD) analysis of Impact Stilling Basin has been done by modelling in Ansys Fluent (R15.0) software. Six different Models namely M-I, M-II, M-III, M-IV, M-V and M-VI have been modelled by changing the distance between the Impact wall and basin inlet , by changing the gap between the basin floor and impact wall. The distance and gap have been calculated in terms of Equivalent diameter'd'. Values of Turbulent Kinetic Energy, Velocity, Wall Shear Stress at Outlet and Energy losses (Kinetic Energy &Specific Energy) have been calculated and compared to find out the best model for energy dissipation in culvert outlets, pipe outlets and open channels so that there is less chances of scouring downstream of these structures. Three cases of Froude number i.e. 1.85, 2.85 and 3.85 have been taken which results in total 18 cases for the analysis. The results obtained can be used to increase the performance of the USBR Type VI Impact Basin.

# CONTENTS

# LIST OF FIGURES

# LIST OF TABLES

# CHAPTER 1
# INTRODUCTION

Energy dissipation is not only required at downstream of spillway of a dam and barrage but also an important phenomenon to prevent erosion at canal outlets, culvert outlets. The failure or damage of many culverts, pipe outlets and detention basin outlet structures are caused by unchecked erosion. Erosive forces, which are at work in the natural drainage network, are often aggravated by the construction of a highway or by other urban development. Interception and concentration of overland flow and narrower of natural waterways inevitably results in an increased erosion potential. To protect the culvert and adjacent areas, it is sometimes necessary to employ an energy dissipator. Energy dissipators are structures designed to protect downstream areas as well as drainage structures from erosion and scouring by causing energy losses and reducing the velocity of flow to acceptable limits.

## 1.1 Types of Energy Dissipators

As per Hydraulic Engineering Circular 14 (HEC-14) provided by Federal Highway Administration of U.S department of transportation, energy dissipators are grouped into six categories:

- Internal Dissipators
- Stilling Basins
- Streambed Level Dissipators
- Riprap Basins and Aprons
- Drop Structures
- Stilling Wells

*Internal Dissipators*

These are used where there is limited right of way beyond outlet point for energy dissipation. Hence energy dissipation occurs internally inside the culvert by increasing roughness, creating tumbling flow condition. Some examples of internal dissipators are

- USBR Type IX baffled Apron
- Broken-Back Culvert run out section
- Tumbling Flow Box/Circular Culverts

*Stilling Basins*

Stilling basins are also known as external energy dissipators. They are placed at the outlet of a culvert, pipe or at a downstream of spillway and barrage. They contain important elements like chute blocks, baffle blocks, and end-sills designed to create a hydraulic jump in combination with a required tail-water condition. The required tail-water is an important aspect in its design hence velocity leaving the end-sill must be equal to the velocity in the receiving channel. Depending upon minimum & maximum approach Froude numbers ($F_r$) they are categorized as:

**Table 1** Applicable Froude Number Ranges for Stilling Basins

| Type of Stilling Basin | Minimum Approach $F_r$ | Maximum Approach $F_r$ |
|---|---|---|
| USBR Type III | 4.5 | 17 |
| USBR Type IV | 2.5 | 4.5 |
| St. Anthony Falls (SAF) | 1.7 | 17 |

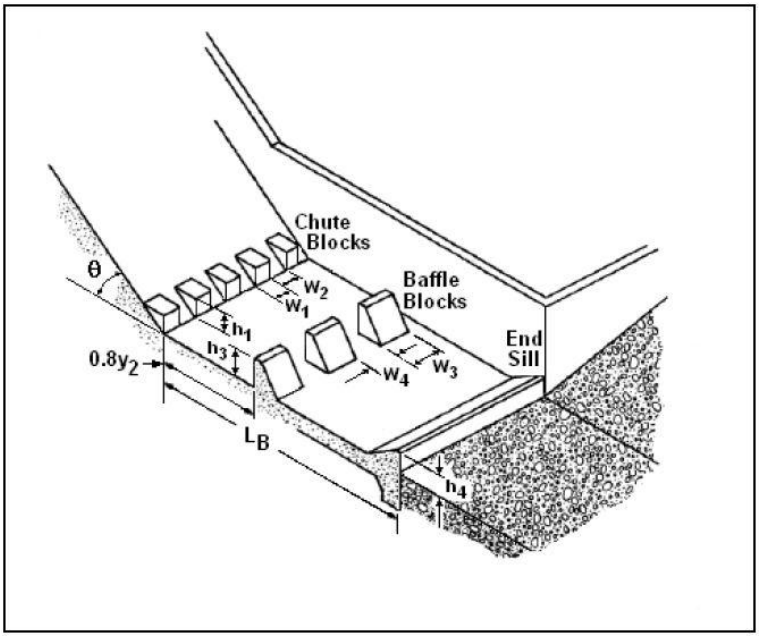


**Figure 1** Showing USBR TYPE III Stilling Basin with chute blocks, baffle blocks and end sill.

*Streambed Level Dissipators*

These are used where culvert outlets are at streambed level and natural flow conditions has to be re-establish downstream of the outlet. The natural gravity flow occurs even when it is not in operation. Some examples of streambed level dissipator:

- Colorado State University (CSU) rigid boundary basin
- Contra Costa basin
- Hook basin
- U.S. Bureau of Reclamation (USBR) Type VI Impact basin

*Riprap Basins and Aprons*

Riprap is a type of stone like material which is used to dissipate energy of flowing water. Riprap basin can be used at outlet of any of the culvert or channel as an energy dissipator. Also it can be used at the exit of another stilling basin or energy dissipator as a secondary dissipator.

*Drop Structures*

Drop structures are commonly used for flow control and energy dissipation. By placing drop structures at certain intervals along the channel, changes a continuous steep slope into a series of mild slopes and vertical drops. Drop Structures prevents the development of erosive velocities rather than controlling the flow. The velocity and kinetic energy gained by the water as it drops over the crest of each structure is dissipated by a specially designed apron or stilling basin. Some examples are

- Straight drop structure
- Box inlet drop structure

*Stilling Wells*

The stilling well can be used in channels with moderate to high concentrations of sand or silt and there is little or no presence of debris. If debris is expected suitable debris-control structures should be used. The highway uses stilling wells at the outfalls of storm drains and pipe down drains where small debris is expected.

## 1.2 U.S. Bureau of Reclamation (USBR) Type VI Impact Basin

As the name suggest it was developed at the U.S Bureau of Reclamation laboratory in 1957.

- It is also referred as hanging baffle type.
- The basin is contained in a box-like structure which is relatively small in size.
- It does not require any tail-water to perform successfully.

- Although mostly used for culvert outlets, it can also be used in case of open channels as well.
- Maximum discharge allowed is 11.33 $m^3$ and maximum velocity allowed is 15m/s

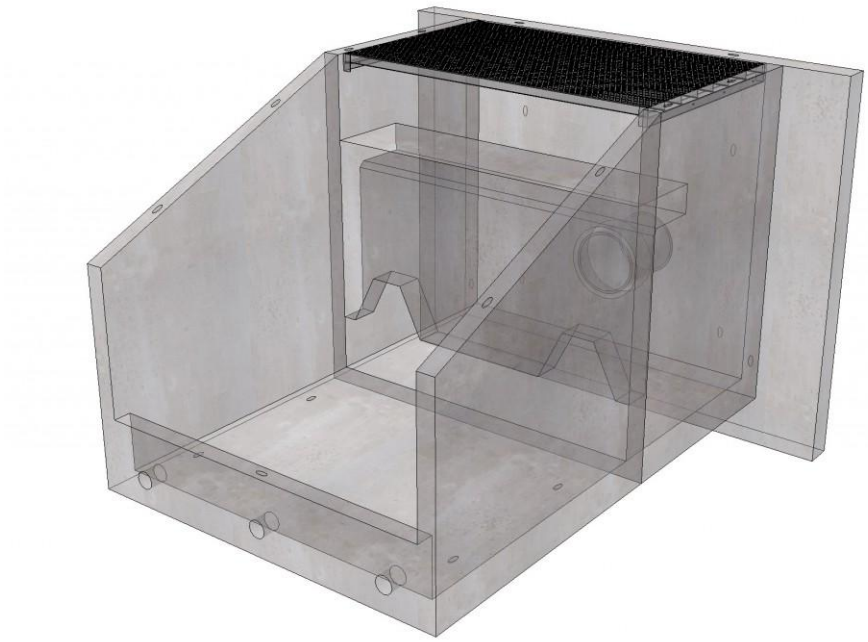

**Figure 2** 3D View of Type VI Impact Basin

*Various Components as per Colorado Department of Transportation (CDOT) Drainage Manual*

Hanging Baffle

Energy dissipation takes place as flow strikes the vertical portion of the hanging baffle and then deflected upstream by the horizontal portion of the baffle and finally hitting the floor, thereby creating horizontal eddies.

Notches In Baffle

Notches are provided to aid in cleaning the basin. The notches provide concentrated jets of water for cleaning.

Equivalent Depth

Equivalent depth is calculated in case of pipe or irregular-shaped conduit. It is that depth in which the cross section flow of pipe is equivalent to a rectangular cross section where the width is twice the depth of flow.

Tail-water

Tail-water depth is not a decisive factor here as in case of hydraulic jump basins. A moderate depth of tail water will improve performance. For best results maximum tail water should not exceed $h_3 + h_2/2$ (See figure 1.3).

Slope

If culvert slope is greater than 15°, a horizontal section of at least four culvert widths should be provided upstream.

End Sill

An end sill with a low-flow drainage slot, 45° wing walls and a cut-off wall should be provided at the end of the basin.

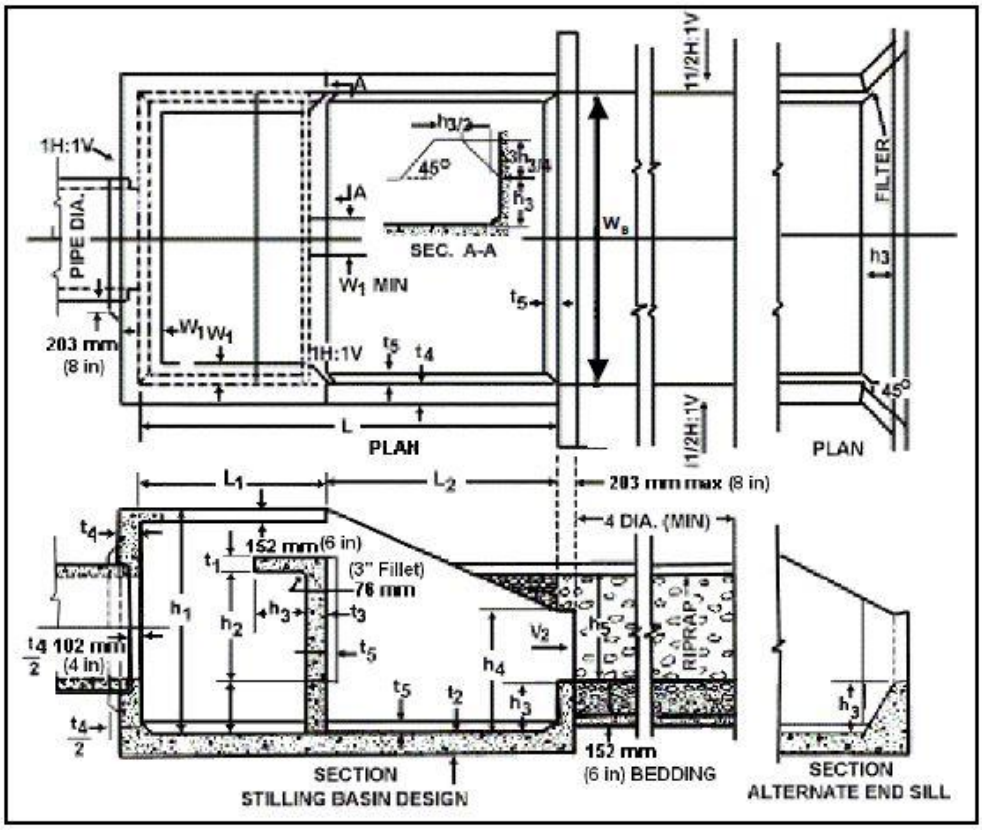


**Figure 3** Plan and cross-section USBR VI Impact Stilling Basin

### 1.2.1 Design Steps for Type VI Impact Basin

1. Calculate Equivalent depth, $d_E$
2. Calculate Input flow parameters like Froude Number (Fr) and Specific Energy ($H_o$)
   $Fr = V/ (gd_E)^{0.5}$, $H_o = d_E + V^2/ (2g)$.
   Where V = velocity entering the basin, g = acceleration due to gravity.
3. Find out basin width, W using graph between Fr and $H_o/W$ (see figure 1.4).
4. Obtain the remaining dimensions of the Basin using the table provided by the CDOT manual (see figure 1.5).

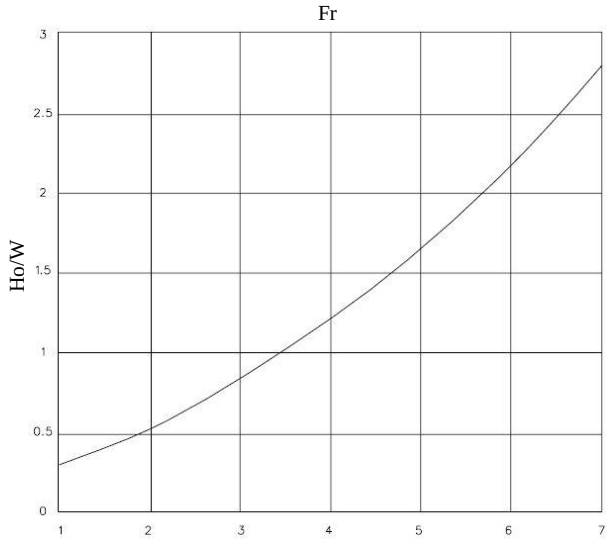


**Figure 4** Design Curve for calculating Width of USBR Type VI Basin

**Table 2** Dimensions of USBR Type VI Impact Basins (In meters)

| W | $h_1$ | $h_2$ | $h_3$ | $h_4$ | L | $L_1$ | $L_2$ |
|---|---|---|---|---|---|---|---|
| 1.0 | 0.79 | 0.38 | 0.17 | 0.43 | 1.40 | 0.59 | 0.79 |
| 1.5 | 1.16 | 0.57 | 0.25 | 0.62 | 2.00 | 0.88 | 1.16 |
| 2.0 | 1.54 | 0.75 | 0.33 | 0.83 | 2.68 | 1.14 | 1.54 |
| 2.5 | 1.93 | 0.94 | 0.42 | 1.04 | 3.33 | 1.43 | 1.93 |
| 3.0 | 2.30 | 1.12 | 0.50 | 1.25 | 4.02 | 1.72 | 2.30 |
| 3.5 | 2.68 | 1.32 | 0.58 | 1.46 | 4.65 | 2.00 | 2.68 |
| 4.0 | 3.12 | 1.51 | 0.67 | 1.67 | 5.33 | 2.28 | 3.08 |
| 4.5 | 3.46 | 1.68 | 0.75 | 1.88 | 6.00 | 2.56 | 3.46 |
| 5.0 | 3.82 | 1.87 | 0.83 | 2.08 | 6.52 | 2.84 | 3.82 |
| 5.5 | 4.19 | 2.03 | 0.91 | 2.29 | 7.29 | 3.12 | 4.19 |
| 6.0 | 4.60 | 2.25 | 1.00 | 2.50 | 7.98 | 3.42 | 4.60 |

## 1.3 Assumptions in Dissertation

1. The shape and size of the standard USBR Type VI Impact basin model has been modified as per convenience to keep the analysis simple and easy to model in Design Modular of Ansys Fluent Software.
2. No Notches have been provided in the baffle wall of CFD Model because cleaning is not important in the study.
3. Two phase flow i.e. 'air' and 'water' is considered and the effect of solid is not considered.
4. The whole study is on **Ansys Fluent (R15.0)** software as developing a physical model in lab is more costly and less precise.
5. Scour hole depth and scouring of graded sand & silt have not been calculated in the as it requires very high level of understanding of software.

## 1.4 Ansys Fluent

Ansys is a computer aided software developed by Ansys Inc. an American company founded by John A. Swanson in the year 1970. It's Head quarter is located in township of Cecil Pennsylvania United States. Ansys provides a suite of software which allows us to do engineering simulation of real life problems in the field of fluid dynamics, Structural mechanics, Electromagnetic, Hydrodynamics and many more.

Fluent is one such software which uses mathematical tool Computation Fluid Dynamics and simulates real life problems related to fluid-structure interactions, Aerodynamics and various other fields related to fluid dynamics. Summary of steps performed during simulation using Fluent are:

- *Geometry*: Geometry construction and defining the fluid region is the first step to simulate and solve any problem. It is done using Design Modular.
- *Meshing (ICEM CFD)*: This is the second step where the fluid domain is broken down into small nodes using Finite Element Method (FEM).
- *Setup*: This is the most important step in the analysis of the problem. Here the initial flow conditions, boundary conditions, type of model, phases etc are input. If a problem is not correctly setup then inaccurate results will come.

- *Solution*: It is the second last step in the analysis. Here solution is initialized and step-size, number of iterations and number of time steps of analysis is selected. Lastly analysis is run and allowed to converge.
- *Results*: This is the final step of analysis. It is also called post-analysis of the problem. Here all streamlines and graphs of various parameters like velocity, pressure, phase , turbulent kinetic energy, wall shear stress etc are plotted and studied in detail.

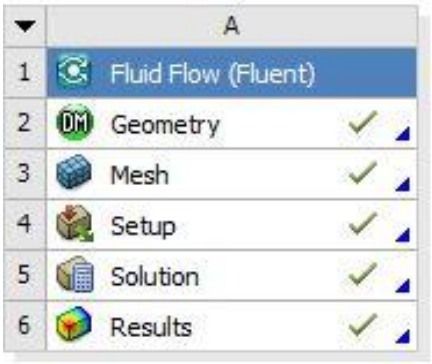


**Figure 5** Various steps in analysis of a problem using Fluent

## 1.5 Objective of Dissertation

1. To validate the experimental investigation done by **H.L Tiwari** and **Arun Goel** on impact stilling basin by developing a model of the basin in Ansys fluent software and performing the analysis on the same.
2. To study the behaviour of flow in a Impact stilling basin when the distance between the hanging baffle and inlet is increased and also when the gap between the baffle wall and the basin floor is increased.
3. To have a good knowledge and understanding of fluent software.
4. To evaluate the performance of impact basin using parameters other than used in the experimental investigation.

## 1.6 Organisation of Dissertation

The dissertation is subdivided into six chapters. *Chapter 1* introduces the topic and discusses the assumptions and aim of the study. *Chapter 2* presents the review of various literatures available on this topic. The methodology and numerical data involved in this dissertation work are discussed in *Chapter 3* and *Chapter 4* respectively. The results and the discussions are enlisted in *Chapter 5*. Finally in *Chapter 6*, conclusion of the study and scope of future work are discussed.

# CHAPTER 2

# LITRATURE REVIEW

Verma D.V.S et al. [1] An experimental study was done to improve the performance and to shorten the basin length of USBR Type VI impact stilling basin. An effort was done to bring the basin floor at the invert level of the pipe outlet. For this various experiments were performed in lab with Froude number ranges from 1.70 to 5.50. Wedge shape splitter blocks, end sill and baffle wall of different sizes were used at different locations from pipe outlet (Pipe outlet of diameter 7.5cm and 10cm was used). To evaluate the performance a non-dimensional number called performance number (PN) was calculated which includes scour as well as flow parameters. PN was defined as ratio of scour Froude number ($F_{dm}$) and tangent to the parabola (Tanα) at the base of the maximum scour located as downstream of end sill($PN = \frac{F_{dm}}{Tan\alpha}$). All the dimensions were transformed into a factor of equivalent diameter of pipe (d). It was concluded form the experiment performed that new models **M, M-I, M-II** were developed which had a better PN than typical USBR Type VI and also the length of the basin reduced to 25% with smaller tail-water depth.

**Table 2** Comparison of USBR with new Models

| Model Type | Length | PN (Fr =1.70) | PN (Fr =2.70) | PN (Fr = 3.70) |
|---|---|---|---|---|
| USBR Type VI | 8d | 0.39 | 0.31 | 0.36 |
| M | 4.5d | 0.47 | 0.77 | 0.59 |
| M-I | 4.5d | 1.11 | 0.50 | 0.76 |
| M-II | 4.5d | 1.27 | 0.59 | 0.91 |

Goel A et al. [2] An experimental study consist of 57 tests were carried out in a lab for the enhancement of energy dissipation caused by Impact stilling basin. Also these experiments were performed to find out the effect of size, shape and position of impact wall and gap between impact wall and basin floor. All the experiments were carried in a flume size 25m x 0.95 m x 1m deep with three cases of Froude number viz. 1.85, 2.85 & 3.85. To evaluate the performance a non-dimensional number called Performance Index (PI) was calculated which is a function of channel velocity (V), the maximum depth of scour ($d_m$) and its location from the end sill ($d_s$) ($PI = \frac{V \times d_s}{d_m \times \sqrt{g\frac{\rho_s - \rho_w}{\rho_w} d_{50}}}$). All the dimensions of the Impact stilling were

calculated in terms of equivalent diameter (d). It was concluded that size, shape and location of impact wall affects the flow condition which ultimately affects the scour downstream of the basin. Higher the Perform Index higher the energy dissipation and the highest PI was observed with impact wall of size 1.5d x3d at a distance of 4d from the pipe outlet with length of basin reduced up to 30% as compared to USBR type VI stilling basin and with a gap of 1d between wall and basin floor.

Tiwari H.L et al. [3] A total of 24 test run were performed in a lab to find out the appropriate size of impact wall used in Impact stilling basin for energy dissipation. Seven different models other than base model of USBR Type VI Impact Basin with different size of impact wall located at suitable distance from pipe outlet for three cases of Froude number i.e. 1.85, 2.85 and 3.85 were tested and performance of each model was evaluated using a non dimensional number named Performance Index (PI). Size of impact wall was taken in terms of equivalent diameter (d). It was concluded that impact wall of size 1.5d x 3d has a better performance than other size of walls viz. 1d x 2.2d, 0.75d x1.5d and 1.25d x 2.5d. It was thought that this better performance is due to increased surface area skin friction which dissipates more energy. It was also found that the length of USBR Type VI Impact basin can be reduced up to 29%.

Tiwari H.L [4] A total 12 tests were carried out to find the appropriate gap between the impact wall and basin floor so that maximum energy is dissipated. Four different models with same size of impact wall and at a same distance from the pipe outlet were tested as the distance between the hanging baffle impact wall and basin floor is changed. The pipe outlet was kept at a distance equal to one equivalent diameter (1d). Gap was increased from 0.5d then to 0.75d then to 1d and finally to 1.5d keeping all the parameters same. The basin was followed erodible bed of coarse sand. The erodible bed was used to find out the scouring parameters i.e. maximum depth of scour ($d_m$) and distance of scour hole from end sill ($d_s$). A non dimensional number called as Performance Index was calculated which is the function of grain Froude number and scouring parameters $d_m$ and $d_s$. It was observed that as the gap between impact wall and basin floor was increased from 0.5d to 1d the value of performance index increased but as the gap was increased to 1.5d the value of performance index decreased. Hence it was concluded that the best performance of impact basin was observed when the gap was 1d.

Thomson P.L et al. [5] It was a technical report titled as Hydraulic Engineering Circular No. 14 (HEC-14) for the hydraulic design of energy dissipators for culverts and channels published by the Federal Highway Administration of National Highway Institute on July 2006.The purpose of this report was to provide information regarding design of energy dissipator and help in reducing the energy dissipation problems in culvert outlets and open channels. The starting chapters of this report discusses the hazards of erosion in culvert outlets and open channel, choosing suitable energy dissipator and design steps in designing an energy dissipator. Article 9.3 of chapter 9 focussed on the design aspects of USBR Type VI Impact basin. It also states the advantages of USBR Type VI basin over conventional Hydraulic Jump basin and limitations of using it in terms of velocity, Froude number and boulder size.

# CHAPTER 3
# METHODOLOGY

## 3.1 Numerical Method

Modelling and analysis of Impact Stilling Basin has been done in Ansys fluent software. This software uses numerical methods like Finite Element Analysis (FEA) for simulation purpose. The process of numerical simulation involves three basic steps:

1. Pre-Processing
    - Setting up of geometry and fluid domain.
    - Discretization or creation of meshing for geometry and fluid domain.
    - Setting up of problem by defining the initial conditions, boundary condition, choosing appropriate equation model and initializing.
2. Solver
    - Software uses suitable mathematical equations and performs iterations over and over until the desired accuracy is achieved.
3. Post-Processing
    - Results are presented in form of graphs, animations and are analysed.

## 3.2 Geometry Setup

The R 15.0 version of Ansys workbench has its own software for drawing of geometry, it is called Design Modular. There are total six different models of Impact Stilling basin whose geometry has been drawn in design modular. All the models are drawn in shape of a rectangular box with length = 7d (65.1cm), width = 6.3d (58.6cm), and height = 5.2d (50cm) where‘d’ is the equivalent diameter of pipe outlet (d =9.3cm). Also the inlet to all models is a rectangular inlet of size 10.8cm x 6.3cm kept at one equivalent diameter above the basin floor. At outlet triangular end sill is provided of size 1d x 1d (9.3 x 9.3 cm) with 45°. The impact wall size in each case is taken as 1.5d x 3d x 0.3d (13.95 x 2 7.9 x 2.79). Six models are differentiated by varying the distance between the impact wall and inlet and by changing the gap between the wall and the basin floor. The details of each model are given below in the table.

**Table 3** Different type of Models of Impact Stilling Basin

| S.No. | Model name | Impact wall size | Distance from inlet | Gap between wall and basin floor |
|---|---|---|---|---|
| 1 | M-I | 1.5d x 3d | 2d | 1d |
| 2 | M-II | 1.5d x 3d | 3d | 1d |
| 3 | M-III | 1.5d x 3d | 4d | 1d |
| 4 | M-IV | 1.5d x 3d | 4d | 0.75d |
| 5 | M-V | 1.5d x 3d | 4d | 0.5d |
| 6 | M-VI | 1.5d x 3d | 4d | 1.5d |

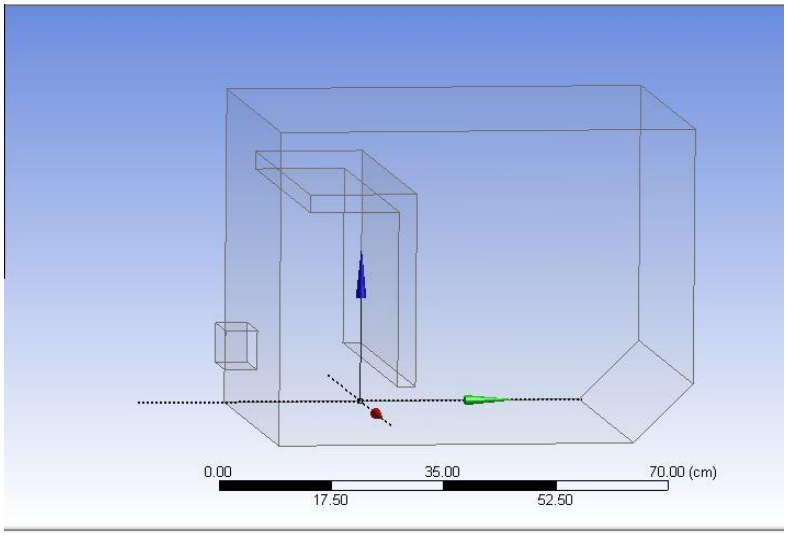


**Figure 6** Geometry of Model -I drawn in Design Modular

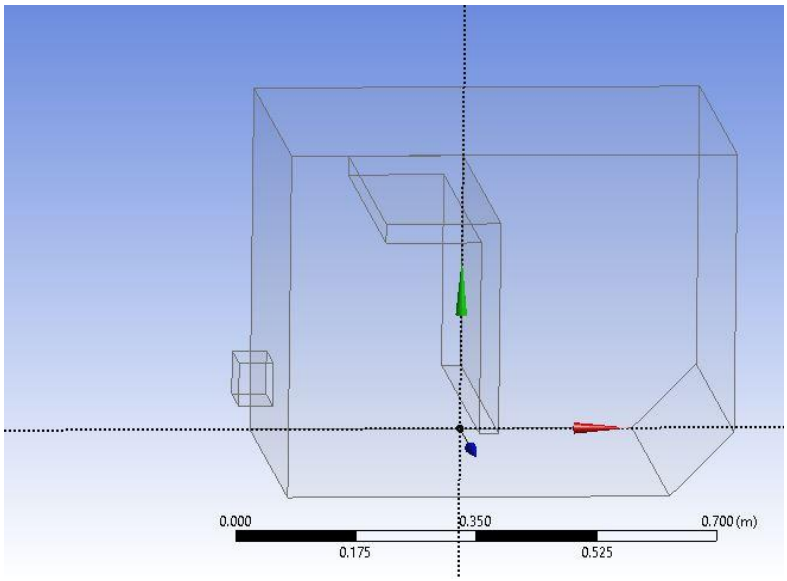


**Figure 7** Geometry of Model -II drawn in Design Modular

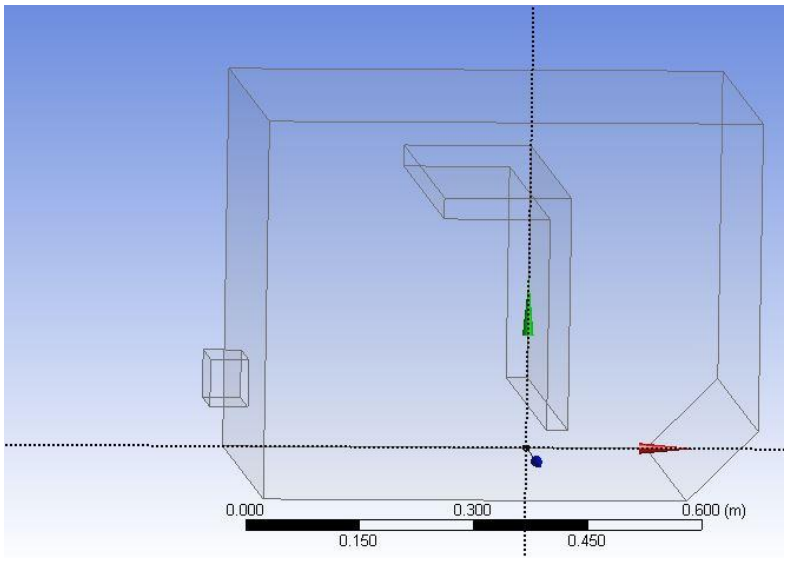


**Figure 8** Geometry of Model -III drawn in Design Modular

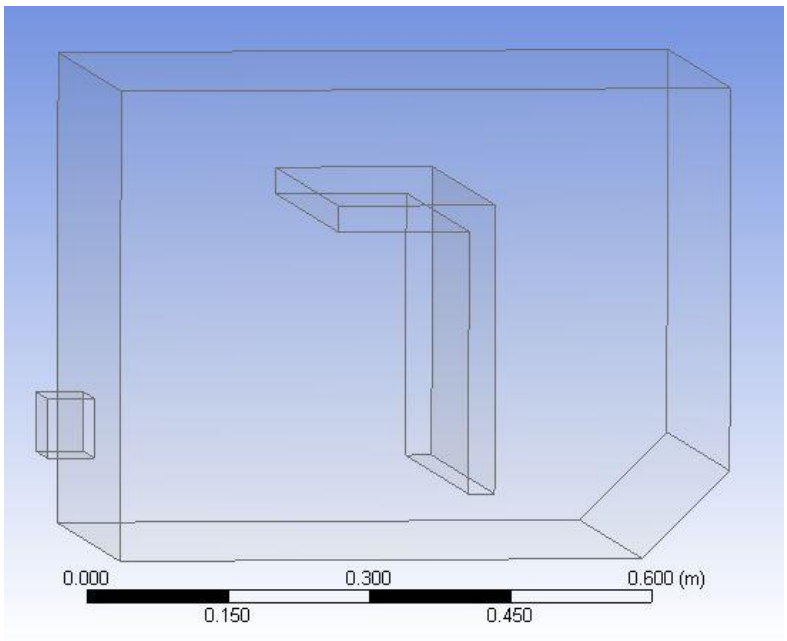


**Figure 9** Geometry of Model -IV drawn in Design Modular

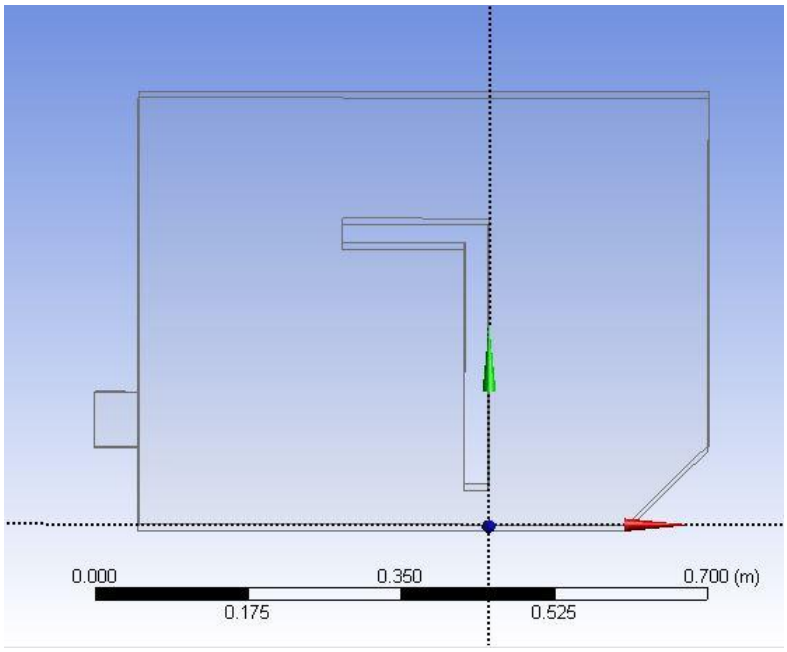


**Figure 10** Geometry of Model -V drawn in Design Modular

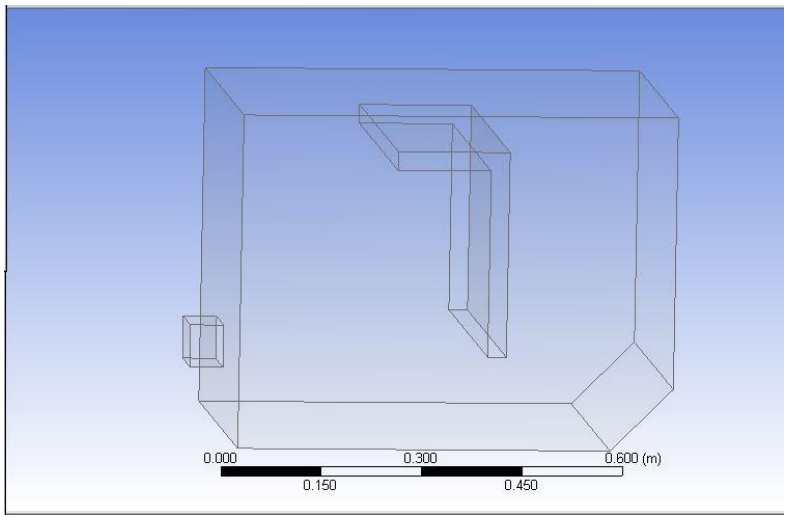


**Figure 11** Geometry of Model -VI drawn in Design Modular

## 3.3 Meshing

The meshing has been done by Ansys ICEM CFD software which is a part of Ansys workbench. The meshing details of all the six models have been kept same. Advance size function is on choosing '*proximity and curvature'*, relevance centre '*fine*', smoothing '*high*', Maximum *8* Inflation layers are used with *smooth* transition and growth rate of *1.4* and *Tetrahedron method* in assembly meshing.

Details of "Mesh"

| | |
|---|---|
| **Defaults** | |
| Physics Preference | CFD |
| Solver Preference | Fluent |
| Relevance | 0 |
| **Sizing** | |
| Use Advanced Size Function | On: Proximity and C... |
| Relevance Center | Fine |
| Smoothing | High |
| Curvature Normal Angle | Default (18.0 °) |
| Num Cells Across Gap | Default (3) |
| Proximity Size Function Sour... | Edges |
| Min Size | Default (2.3758e-00... |
| Proximity Min Size | Default (2.3758e-00... |
| Max Size | Default (3.041e-002 ... |
| Growth Rate | Default (1.20 ) |
| Minimum Edge Length | 2.79e-002 m |
| **Inflation** | |
| Use Automatic Inflation | None |
| Inflation Option | Smooth Transition |
| Transition Ratio | 0.272 |
| Maximum Layers | 8 |
| Growth Rate | 1.4 |
| View Advanced Options | No |
| **Assembly Meshing** | |
| Method | Tetrahedrons |
| Feature Capture | Program Controlled |
| Tessellation Refinement | Program Controlled |

**Figure 12** Details of Mesh

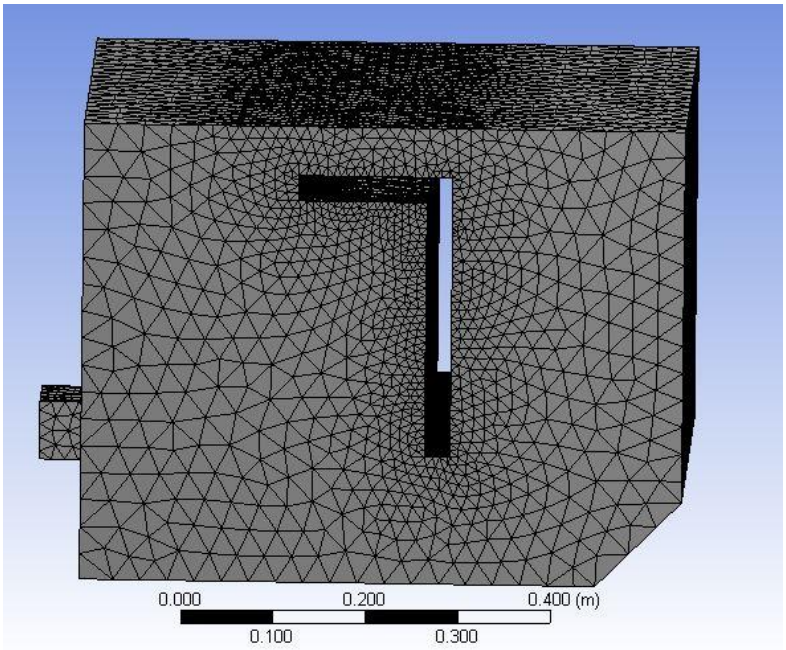


**Figure 13** Mesh Diagram drawn in ICEM CFD

## 3.4 Fluent Setup

The most important aspect in the simulation process is setting up of the problem in fluent software. In fluent launcher 3D, Double Precision and Serial Processing option is selected and setup is started. The first option that opens up in setup is *General* in which pressure type solver, absolute velocity formulation, transient time and direction of gravity in –ve Y direction are selected. The next step is to choose *Models* in which multiphase, number of eulerian phases 2 and implicit scheme is selected. Also 'k-ε' viscous model is selected. The third step is to select fluid from *Materials*, as air is already present new fluid water-liquid is added from database of Ansys. Next step is to assign primary phase (i.e. Phase I) to air and secondary phase (i.e. Phase II) to water from *Phases* option. The fifth step is to input reference pressure location and select specified operating density in the *Cell Zone Condition* option. Sixth step is the most important step as boundary conditions and initial conditions are entered and hence the option is named as *Boundary Conditions*. Inlet is taken as velocity inlet and velocity of flow entering the basin is entered and 'intensity and hydraulic diameter' specification method is chosen. Also phase II volume fraction is taken as 1 to insure only water entered from the inlet. Outlet is taken as pressure outlet.

Finally solution is initialized using *Hybrid Initialization* method and after that liquid region is patched using patch option which ensures that at the start of the simulation which portion is filled with water and which portion of basin is filled with air. The last option is *Run Calculation* where time step size 1 sec, number of time steps 40 and maximum iteration per time step 5 are entered and solution is allowed to run.

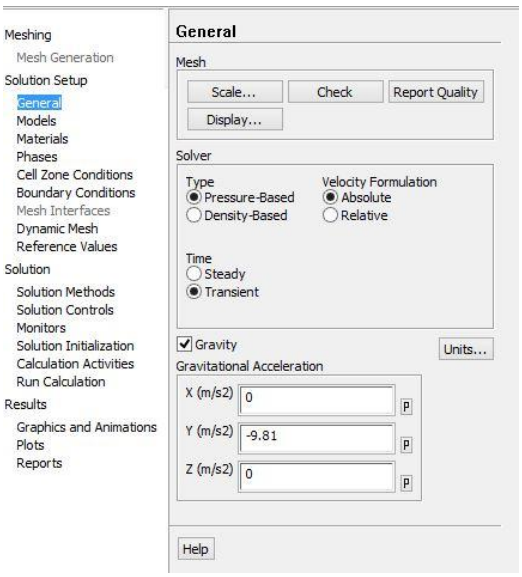


**Figure 14** Different options in fluent setup

### 3.4.1 Equations Used By Fluent

*Reynolds Averaged Navier-Stokes Equations (RANS)*

$$\frac{\partial \rho}{\partial t} + \frac{\partial u_i}{\partial x_i} = 0 \quad \text{.....Eq.3.1}$$

$$\frac{\partial(\rho u_i)}{\partial t} + \frac{\partial(\rho u_i u_j)}{\partial x_j} = -\frac{\partial p}{\partial x_i} + \frac{\partial}{\partial x_j}\mu\left(\frac{\partial u_i}{\partial x_j} + \frac{\partial u_j}{\partial x_i}\right) + -\frac{\partial(\rho \bar{u}_i{}' \bar{u}_j{}')}{\partial x_j} \quad \text{……Eq.3.2}$$

Where $\bar{u}'\bar{v}'$ represents mean and fluctuating component of velocity vector, vector $u_{i,j}$ is velocity, vector $x_{i,j}$ is position, t is time, p is pressure, ρ is density and $\mu$ =dynamic viscosity.

*Transport Equations for the Standard k-ε Model*

$$\frac{\partial}{\partial t}(\rho k) + \frac{\partial}{\partial t}(\rho k u_i) = \frac{\partial}{\partial x_j}\left[\left(\mu + \frac{\mu_t}{\sigma_k}\right)\frac{\partial k}{\partial x_j}\right] + G_k + G_b - \rho\varepsilon - Y_M + S_k \quad \text{..Eq.3.3}$$

$$\frac{\partial}{\partial t}(\rho \varepsilon) + \frac{\partial}{\partial t}(\rho \varepsilon u_i) = \frac{\partial}{\partial x_j}\left[\left(\mu + \frac{\mu_t}{\sigma_\varepsilon}\right)\frac{\partial k}{\partial x_j}\right] + C_{1\varepsilon}\frac{\varepsilon}{k}(G_k + C_{3\varepsilon}G_b) - C_{2\varepsilon}\rho\frac{\varepsilon^2}{k} + S_\varepsilon \text{..Eq.3.4}$$

In these equations, $G_k$ represents the generation of turbulence kinetic energy due to the mean velocity gradients; $G_b$ is the generation of turbulence kinetic energy due to buoyancy. $Y_M$ represents the contribution of the fluctuating dilatation in compressible turbulence to the overall dissipation rate. $C_{1\varepsilon}$, $C_{2\varepsilon}$ and $C_{3\varepsilon}$ are constants. $\sigma_K$ and $\sigma_\varepsilon$ are the turbulent Prandtl numbers for k and ε respectively. $S_K$ and $S_\varepsilon$ are user-defined source terms.

The turbulent (or eddy) viscosity,$\mu_t$, is computed by combining k and ε as :

$$\mu_t = \rho C_\mu \frac{k^2}{\varepsilon} \quad \text{……Eq.3.5}$$

Where $C_\mu$ is a constant.

The model constants $C_{1\varepsilon}$, $C_{2\varepsilon}$, $C_{3\varepsilon}$, $\sigma_K$ and $\sigma_\varepsilon$ have the following default values

$C_{1\varepsilon}$ =1.44, $C_{2\varepsilon}$ = 1.92, $C_{3\varepsilon}$ = 0.09, $\sigma_K$ = 1.0 and $\sigma_\varepsilon$ = 1.3

These default values have been determined from experiments for fundamental turbulent flows including frequently encountered shear flows like boundary layers, mixing layers and jets as well as for decaying isotropic grid turbulence.

# CHAPTER 4

# NUMERICAL DATA AND CALCULATIONS

## 4.1 Calculation of Equivalent Diameter and Inlet Velocity

Size of Rectangular pipe = 10.8cm x 6.3cm

Equivalent diameter, d = $\sqrt{(\frac{4\times A}{\pi})}$

d = $\sqrt{(\frac{4\times 10.8\times 6.3}{\pi})}$

d = 9.3 cm.

Froude Number, Fr = 1.85

Fr = $\frac{V}{\sqrt{gd}}$ …….Eq.4.1

Where V is inlet velocity, g = acceleration due to gravity = 9.8 m/s$^2$

$V^2 = 1.85^2 \times 9.81 \times 0.093$

V = 1.767 m/s

Similarly for Fr = 2.85, V =2.722 m/s and for Fr = 3.85, V = 3.677 m/s

## 4.2 Data Obtained from Fluent Results

The following tables contain data that is obtained after calculation is completed by fluent software. The Table contains values of Turbulent Kinetic Energy, Velocity at outlet, Energy losses and Shear stress at outlet bottom for six Models M-I, M-II, M-III, M-IV, M-V & M-VI for three cases of Froude number 1.85, 2.85 and 3.85.

**Table 4** Turbulent Kinetic Energy values at Outlet for Fr =1.85

| | **Turbulent Kinetic Energy ($m^2/s^2$) For Fr = 1.85** | | | | | |
|---|---|---|---|---|---|---|
| **$Y_{outlet}$ (m)** | **M-I** | **M-II** | **M-III** | **M-IV** | **M-V** | **M-VI** |
| 0.093 | 0.011 | 0.012 | 0.026 | 0.038 | 0.019 | 0.076 |
| 0.093 | 0.014 | 0.014 | 0.030 | 0.026 | 0.023 | 0.063 |
| 0.093 | 0.011 | 0.033 | 0.046 | 0.041 | 0.025 | 0.070 |
| 0.093 | 0.011 | 0.041 | 0.042 | 0.046 | 0.026 | 0.068 |
| 0.093 | 0.020 | 0.041 | 0.047 | 0.039 | 0.028 | 0.057 |
| 0.093 | 0.024 | 0.037 | 0.044 | 0.039 | 0.031 | 0.060 |
| 0.093 | 0.028 | 0.031 | 0.039 | 0.042 | 0.032 | 0.059 |
| 0.093 | 0.025 | 0.034 | 0.033 | 0.044 | 0.028 | 0.068 |
| 0.093 | 0.026 | 0.028 | 0.033 | 0.044 | 0.023 | 0.079 |
| 0.093 | 0.024 | 0.024 | 0.029 | 0.046 | 0.022 | 0.088 |

| | | | | | | |
|---|---|---|---|---|---|---|
| 0.093 | 0.024 | 0.028 | 0.026 | 0.044 | 0.029 | 0.102 |
| 0.093 | 0.023 | 0.037 | 0.028 | 0.043 | 0.028 | 0.108 |
| 0.093 | 0.022 | 0.033 | 0.031 | 0.040 | 0.023 | 0.107 |
| 0.093 | 0.022 | 0.041 | 0.032 | 0.038 | 0.027 | 0.105 |
| 0.093 | 0.023 | 0.021 | 0.034 | 0.042 | 0.026 | 0.106 |
| 0.093 | 0.023 | 0.021 | 0.040 | 0.035 | 0.026 | 0.098 |
| 0.093 | 0.023 | 0.026 | 0.047 | 0.033 | 0.024 | 0.103 |
| 0.093 | 0.018 | 0.045 | 0.029 | 0.031 | 0.025 | 0.086 |
| 0.093 | 0.014 | 0.047 | 0.036 | 0.022 | 0.026 | 0.062 |
| 0.093 | 0.023 | 0.032 | 0.030 | 0.017 | 0.020 | 0.042 |
| 0.093 | 0.027 | 0.015 | 0.021 | 0.018 | 0.018 | 0.045 |
| 0.117 | 0.022 | 0.036 | 0.073 | 0.083 | 0.016 | 0.108 |
| 0.117 | 0.022 | 0.036 | 0.040 | 0.080 | 0.133 | 0.052 |
| 0.118 | 0.021 | 0.057 | 0.036 | 0.084 | 0.036 | 0.070 |
| 0.118 | 0.034 | 0.049 | 0.076 | 0.024 | 0.120 | 0.076 |
| 0.119 | 0.011 | 0.042 | 0.091 | 0.041 | 0.118 | 0.109 |
| 0.120 | 0.013 | 0.057 | 0.064 | 0.092 | 0.036 | 0.104 |
| 0.120 | 0.038 | 0.058 | 0.070 | 0.079 | 0.037 | 0.114 |
| 0.120 | 0.032 | 0.030 | 0.096 | 0.102 | 0.126 | 0.160 |
| 0.120 | 0.042 | 0.036 | 0.083 | 0.099 | 0.054 | 0.152 |
| 0.120 | 0.014 | 0.024 | 0.076 | 0.051 | 0.064 | 0.104 |
| 0.120 | 0.048 | 0.041 | 0.061 | 0.072 | 0.040 | 0.152 |
| 0.120 | 0.044 | 0.059 | 0.090 | 0.109 | 0.126 | 0.101 |
| 0.120 | 0.024 | 0.078 | 0.110 | 0.110 | 0.069 | 0.159 |
| 0.121 | 0.041 | 0.027 | 0.102 | 0.079 | 0.065 | 0.107 |
| 0.121 | 0.042 | 0.059 | 0.065 | 0.105 | 0.062 | 0.122 |
| 0.121 | 0.047 | 0.073 | 0.112 | 0.109 | 0.044 | 0.119 |
| 0.121 | 0.045 | 0.082 | 0.064 | 0.090 | 0.036 | 0.156 |
| 0.122 | 0.048 | 0.053 | 0.062 | 0.106 | 0.041 | 0.128 |
| 0.122 | 0.026 | 0.042 | 0.082 | 0.111 | 0.050 | 0.157 |
| 0.122 | 0.052 | 0.082 | 0.074 | 0.114 | 0.059 | 0.140 |
| 0.125 | 0.040 | 0.060 | 0.102 | 0.117 | 0.044 | 0.152 |
| 0.139 | 0.050 | 0.092 | 0.117 | 0.050 | 0.041 | 0.134 |
| 0.145 | 0.134 | 0.085 | 0.113 | 0.045 | 0.049 | 0.158 |
| 0.145 | 0.154 | 0.098 | 0.105 | 0.038 | 0.053 | 0.150 |
| 0.146 | 0.153 | 0.095 | 0.072 | 0.058 | 0.043 | 0.117 |
| 0.146 | 0.168 | 0.036 | 0.027 | 0.107 | 0.091 | 0.164 |
| 0.146 | 0.176 | 0.045 | 0.027 | 0.099 | 0.127 | 0.078 |
| 0.146 | 0.166 | 0.066 | 0.085 | 0.057 | 0.023 | 0.067 |
| 0.147 | 0.181 | 0.099 | 0.068 | 0.025 | 0.032 | 0.216 |
| 0.148 | 0.095 | 0.079 | 0.085 | 0.056 | 0.077 | 0.179 |
| 0.148 | 0.085 | 0.079 | 0.064 | 0.052 | 0.107 | 0.216 |
| 0.148 | 0.014 | 0.104 | 0.008 | 0.055 | 0.118 | 0.210 |
| 0.148 | 0.023 | 0.086 | 0.011 | 0.077 | 0.115 | 0.163 |
| 0.148 | 0.190 | 0.096 | 0.007 | 0.029 | 0.051 | 0.160 |
| 0.148 | 0.185 | 0.088 | 0.020 | 0.075 | 0.067 | 0.161 |
| 0.149 | 0.086 | 0.097 | 0.029 | 0.077 | 0.070 | 0.209 |
| 0.149 | 0.087 | 0.108 | 0.019 | 0.069 | 0.068 | 0.176 |

| | | | | | | |
|---|---|---|---|---|---|---|
| 0.149 | 0.094 | 0.106 | 0.030 | 0.065 | 0.105 | 0.212 |
| 0.149 | 0.033 | 0.094 | 0.012 | 0.042 | 0.065 | 0.207 |
| 0.149 | 0.061 | 0.097 | 0.013 | 0.058 | 0.069 | 0.188 |
| 0.150 | 0.097 | 0.108 | 0.130 | 0.049 | 0.074 | 0.205 |
| 0.153 | 0.098 | 0.106 | 0.107 | 0.059 | 0.093 | 0.195 |
| 0.164 | 0.062 | 0.106 | 0.112 | 0.070 | 0.076 | 0.204 |
| 0.170 | 0.080 | 0.097 | 0.102 | 0.067 | 0.072 | 0.192 |
| 0.174 | 0.107 | 0.123 | 0.027 | 0.048 | 0.104 | 0.140 |
| 0.174 | 0.107 | 0.104 | 0.024 | 0.047 | 0.049 | 0.140 |
| 0.175 | 0.104 | 0.093 | 0.010 | 0.102 | 0.119 | 0.215 |
| 0.176 | 0.106 | 0.118 | 0.012 | 0.069 | 0.076 | 0.232 |
| 0.176 | 0.113 | 0.048 | 0.009 | 0.106 | 0.129 | 0.243 |
| 0.176 | 0.138 | 0.047 | 0.101 | 0.078 | 0.035 | 0.242 |
| 0.176 | 0.147 | 0.101 | 0.061 | 0.078 | 0.063 | 0.239 |
| 0.176 | 0.157 | 0.103 | 0.047 | 0.046 | 0.132 | 0.081 |
| 0.176 | 0.125 | 0.101 | 0.120 | 0.067 | 0.096 | 0.068 |
| 0.176 | 0.130 | 0.113 | 0.106 | 0.047 | 0.129 | 0.214 |
| 0.176 | 0.136 | 0.114 | 0.111 | 0.079 | 0.135 | 0.219 |
| 0.177 | 0.124 | 0.113 | 0.115 | 0.046 | 0.119 | 0.237 |
| 0.177 | 0.159 | 0.122 | 0.121 | 0.070 | 0.141 | 0.216 |
| 0.177 | 0.139 | 0.118 | 0.111 | 0.064 | 0.115 | 0.216 |
| 0.177 | 0.133 | 0.100 | 0.102 | 0.072 | 0.107 | 0.220 |
| 0.178 | 0.132 | 0.109 | 0.089 | 0.052 | 0.096 | 0.235 |
| 0.178 | 0.123 | 0.077 | 0.085 | 0.052 | 0.141 | 0.226 |
| 0.178 | 0.129 | 0.109 | 0.120 | 0.115 | 0.115 | 0.227 |
| 0.187 | 0.149 | 0.100 | 0.116 | 0.114 | 0.141 | 0.232 |
| 0.193 | 0..132 | 0.101 | 0.120 | 0.117 | 0.116 | 0.208 |

**Table 5** Turbulent Kinetic Energy values at Outlet for Fr =2.85

| | **Turbulent Kinetic Energy ($m^2/s^2$) For Fr = 2.85** | | | | | |
|---|---|---|---|---|---|---|
| **$Y_{outlet}$ (m)** | **M-I** | **M-II** | **M-III** | **M-IV** | **M-V** | **M-VI** |
| 0.093 | 0.042 | 0.049 | 0.039 | 0.036 | 0.041 | 0.061 |
| 0.093 | 0.043 | 0.046 | 0.038 | 0.026 | 0.026 | 0.044 |
| 0.093 | 0.040 | 0.046 | 0.037 | 0.041 | 0.039 | 0.074 |
| 0.093 | 0.041 | 0.045 | 0.036 | 0.040 | 0.042 | 0.082 |
| 0.093 | 0.019 | 0.044 | 0.135 | 0.036 | 0.044 | 0.084 |
| 0.093 | 0.024 | 0.037 | 0.130 | 0.037 | 0.044 | 0.093 |
| 0.093 | 0.029 | 0.036 | 0.129 | 0.039 | 0.045 | 0.120 |
| 0.093 | 0.027 | 0.032 | 0.129 | 0.043 | 0.042 | 0.133 |
| 0.093 | 0.029 | 0.030 | 0.126 | 0.046 | 0.052 | 0.117 |
| 0.093 | 0.028 | 0.028 | 0.121 | 0.050 | 0.052 | 0.084 |
| 0.093 | 0.029 | 0.027 | 0.123 | 0.045 | 0.052 | 0.086 |
| 0.093 | 0.030 | 0.025 | 0.022 | 0.040 | 0.043 | 0.117 |
| 0.093 | 0.029 | 0.023 | 0.026 | 0.036 | 0.042 | 0.125 |
| 0.093 | 0.025 | 0.023 | 0.025 | 0.033 | 0.033 | 0.117 |

| | | | | | | |
|---|---|---|---|---|---|---|
| 0.093 | 0.030 | 0.022 | 0.020 | 0.031 | 0.033 | 0.103 |
| 0.093 | 0.029 | 0.020 | 0.004 | 0.029 | 0.034 | 0.084 |
| 0.093 | 0.026 | 0.018 | 0.003 | 0.029 | 0.033 | 0.079 |
| 0.093 | 0.019 | 0.017 | 0.003 | 0.030 | 0.033 | 0.066 |
| 0.093 | 0.015 | 0.017 | 0.003 | 0.025 | 0.033 | 0.045 |
| 0.093 | 0.026 | 0.015 | 0.002 | 0.020 | 0.028 | 0.032 |
| 0.093 | 0.029 | 0.011 | 0.002 | 0.018 | 0.028 | 0.032 |
| 0.117 | 0.024 | 0.031 | 0.041 | 0.044 | 0.047 | 0.080 |
| 0.117 | 0.024 | 0.022 | 0.003 | 0.036 | 0.038 | 0.040 |
| 0.118 | 0.024 | 0.082 | 0.003 | 0.048 | 0.050 | 0.049 |
| 0.118 | 0.036 | 0.086 | 0.061 | 0.023 | 0.029 | 0.056 |
| 0.119 | 0.011 | 0.062 | 0.069 | 0.028 | 0.028 | 0.082 |
| 0.120 | 0.012 | 0.073 | 0.131 | 0.039 | 0.042 | 0.122 |
| 0.120 | 0.034 | 0.093 | 0.058 | 0.045 | 0.044 | 0.116 |
| 0.120 | 0.026 | 0.055 | 0.045 | 0.051 | 0.054 | 0.156 |
| 0.120 | 0.045 | 0.091 | 0.056 | 0.045 | 0.051 | 0.143 |
| 0.120 | 0.114 | 0.078 | 0.053 | 0.033 | 0.042 | 0.145 |
| 0.120 | 0.158 | 0.042 | 0.133 | 0.041 | 0.044 | 0.131 |
| 0.120 | 0.151 | 0.088 | 0.061 | 0.058 | 0.054 | 0.163 |
| 0.120 | 0.022 | 0.063 | 0.048 | 0.064 | 0.061 | 0.153 |
| 0.121 | 0.060 | 0.105 | 0.057 | 0.040 | 0.043 | 0.157 |
| 0.121 | 0.157 | 0.037 | 0.050 | 0.057 | 0.059 | 0.108 |
| 0.121 | 0.146 | 0.046 | 0.041 | 0.072 | 0.075 | 0.131 |
| 0.121 | 0.168 | 0.049 | 0.058 | 0.041 | 0.042 | 0.125 |
| 0.122 | 0.168 | 0.027 | 0.056 | 0.070 | 0.072 | 0.123 |
| 0.122 | 0.220 | 0.109 | 0.078 | 0.057 | 0.062 | 0.133 |
| 0.122 | 0.147 | 0.061 | 0.059 | 0.062 | 0.050 | 0.108 |
| 0.125 | 0.137 | 0.039 | 0.081 | 0.046 | 0.059 | 0.122 |
| 0.139 | 0.154 | 0.047 | 0.103 | 0.074 | 0.048 | 0.115 |
| 0.145 | 0.131 | 0.064 | 0.102 | 0.053 | 0.073 | 0.167 |
| 0.145 | 0.152 | 0.111 | 0.001 | 0.079 | 0.074 | 0.157 |
| 0.146 | 0.141 | 0.059 | 0.046 | 0.069 | 0.064 | 0.122 |
| 0.146 | 0.157 | 0.040 | 0.015 | 0.048 | 0.063 | 0.191 |
| 0.146 | 0.175 | 0.031 | 0.011 | 0.064 | 0.051 | 0.070 |
| 0.146 | 0.145 | 0.071 | 0.103 | 0.060 | 0.060 | 0.065 |
| 0.147 | 0.171 | 0.052 | 0.084 | 0.061 | 0.066 | 0.202 |
| 0.148 | 0.125 | 0.043 | 0.003 | 0.027 | 0.053 | 0.186 |
| 0.148 | 0.127 | 0.129 | 0.052 | 0.036 | 0.151 | 0.194 |
| 0.148 | 0.113 | 0.047 | 0.093 | 0.095 | 0.070 | 0.198 |
| 0.148 | 0.016 | 0.081 | 0.003 | 0.122 | 0.090 | 0.201 |
| 0.148 | 0.071 | 0.073 | 0.106 | 0.066 | 0.069 | 0.191 |
| 0.148 | 0.092 | 0.212 | 0.109 | 0.130 | 0.079 | 0.169 |
| 0.149 | 0.105 | 0.122 | 0.093 | 0.115 | 0.094 | 0.194 |
| 0.149 | 0.120 | 0.156 | 0.108 | 0.133 | 0.066 | 0.149 |
| 0.149 | 0.087 | 0.088 | 0.102 | 0.112 | 0.165 | 0.179 |

| | | | | | | |
|---|---|---|---|---|---|---|
| 0.149 | 0.124 | 0.038 | 0.110 | 0.073 | 0.159 | 0.195 |
| 0.149 | 0.137 | 0.052 | 0.102 | 0.105 | 0.156 | 0.205 |
| 0.150 | 0.199 | 0.191 | 0.104 | 0.106 | 0.168 | 0.159 |
| 0.153 | 0.187 | 0.201 | 0.106 | 0.128 | 0.160 | 0.196 |
| 0.164 | 0.145 | 0.157 | 0.107 | 0.132 | 0.159 | 0.232 |
| 0.170 | 0.063 | 0.109 | 0.109 | 0.103 | 0.170 | 0.231 |
| 0.174 | 0.153 | 0.122 | 0.104 | 0.155 | 0.168 | 0.149 |
| 0.174 | 0.126 | 0.202 | 0.101 | 0.145 | 0.140 | 0.165 |
| 0.175 | 0.178 | 0.101 | 0.103 | 0.100 | 0.168 | 0.249 |
| 0.176 | 0.101 | 0.164 | 0.110 | 0.100 | 0.175 | 0.244 |
| 0.176 | 0.075 | 0.139 | 0.074 | 0.144 | 0.125 | 0.239 |
| 0.176 | 0.189 | 0.121 | 0.102 | 0.189 | 0.138 | 0.252 |
| 0.176 | 0.151 | 0.168 | 0.037 | 0.167 | 0.191 | 0.221 |
| 0.176 | 0.173 | 0.113 | 0.130 | 0.123 | 0.185 | 0.080 |
| 0.176 | 0.205 | 0.184 | 0.088 | 0.125 | 0.206 | 0.076 |
| 0.176 | 0.204 | 0.143 | 0.079 | 0.141 | 0.120 | 0.193 |
| 0.176 | 0.135 | 0.135 | 0.107 | 0.184 | 0.086 | 0.252 |
| 0.177 | 0.134 | 0.132 | 0.105 | 0.111 | 0.197 | 0.252 |
| 0.177 | 0.091 | 0.103 | 0.110 | 0.204 | 0.181 | 0.241 |
| 0.177 | 0.188 | 0.147 | 0.102 | 0.185 | 0.122 | 0.219 |
| 0.177 | 0.148 | 0.032 | 0.104 | 0.163 | 0.106 | 0.188 |
| 0.178 | 0.163 | 0.104 | 0.200 | 0.137 | 0.102 | 0.205 |
| 0.178 | 0.226 | 0.163 | 0.201 | 0.129 | 0.110 | 0.246 |
| 0.178 | 0.081 | 0.172 | 0.101 | 0.166 | 0.101 | 0.269 |
| 0.187 | 0.168 | 0.157 | 0.123 | 0.101 | 0.117 | 0.206 |
| 0.193 | 0.185 | 0.110 | 0.011 | 0.112 | 0.094 | 0.230 |

**Table 6** Turbulent Kinetic Energy values at Outlet for Fr =3.85

| | **Turbulent Kinetic Energy ($m^2/s^2$) For Fr = 3.85** | | | | | |
|---|---|---|---|---|---|---|
| **$Y_{outlet}$ (m)** | **M-I** | **M-II** | **M-III** | **M-IV** | **M-V** | **M-VI** |
| 0.093 | 0.012 | 0.021 | 0.023 | 0.035 | 0.034 | 0.071 |
| 0.093 | 0.015 | 0.025 | 0.027 | 0.025 | 0.042 | 0.053 |
| 0.093 | 0.010 | 0.038 | 0.041 | 0.047 | 0.047 | 0.081 |
| 0.093 | 0.011 | 0.043 | 0.060 | 0.052 | 0.054 | 0.092 |
| 0.093 | 0.023 | 0.038 | 0.069 | 0.056 | 0.060 | 0.098 |
| 0.093 | 0.030 | 0.036 | 0.060 | 0.064 | 0.060 | 0.116 |
| 0.093 | 0.032 | 0.043 | 0.068 | 0.067 | 0.059 | 0.153 |
| 0.093 | 0.031 | 0.048 | 0.082 | 0.076 | 0.053 | 0.167 |
| 0.093 | 0.035 | 0.055 | 0.083 | 0.083 | 0.046 | 0.149 |
| 0.093 | 0.037 | 0.068 | 0.078 | 0.095 | 0.044 | 0.112 |
| 0.093 | 0.043 | 0.073 | 0.074 | 0.092 | 0.053 | 0.089 |
| 0.093 | 0.049 | 0.067 | 0.078 | 0.079 | 0.052 | 0.094 |
| 0.093 | 0.047 | 0.053 | 0.081 | 0.069 | 0.047 | 0.117 |

| | | | | | | |
|---|---|---|---|---|---|---|
| 0.093 | 0.028 | 0.047 | 0.074 | 0.061 | 0.048 | 0.123 |
| 0.093 | 0.047 | 0.037 | 0.061 | 0.053 | 0.047 | 0.111 |
| 0.093 | 0.041 | 0.028 | 0.054 | 0.042 | 0.049 | 0.090 |
| 0.093 | 0.033 | 0.033 | 0.058 | 0.034 | 0.048 | 0.085 |
| 0.093 | 0.020 | 0.042 | 0.053 | 0.033 | 0.049 | 0.077 |
| 0.093 | 0.016 | 0.042 | 0.049 | 0.028 | 0.044 | 0.060 |
| 0.093 | 0.026 | 0.026 | 0.028 | 0.025 | 0.034 | 0.045 |
| 0.093 | 0.028 | 0.019 | 0.070 | 0.024 | 0.033 | 0.040 |
| 0.117 | 0.024 | 0.025 | 0.032 | 0.067 | 0.028 | 0.085 |
| 0.117 | 0.029 | 0.023 | 0.030 | 0.062 | 0.058 | 0.047 |
| 0.118 | 0.026 | 0.058 | 0.088 | 0.041 | 0.058 | 0.055 |
| 0.118 | 0.035 | 0.041 | 0.083 | 0.028 | 0.034 | 0.062 |
| 0.119 | 0.011 | 0.040 | 0.054 | 0.028 | 0.029 | 0.084 |
| 0.120 | 0.012 | 0.054 | 0.015 | 0.076 | 0.061 | 0.133 |
| 0.120 | 0.038 | 0.039 | 0.079 | 0.034 | 0.064 | 0.121 |
| 0.120 | 0.030 | 0.077 | 0.109 | 0.079 | 0.038 | 0.160 |
| 0.120 | 0.047 | 0.083 | 0.102 | 0.100 | 0.066 | 0.145 |
| 0.120 | 0.014 | 0.117 | 0.053 | 0.035 | 0.070 | 0.168 |
| 0.120 | 0.083 | 0.062 | 0.108 | 0.041 | 0.058 | 0.126 |
| 0.120 | 0.062 | 0.049 | 0.100 | 0.091 | 0.039 | 0.195 |
| 0.120 | 0.022 | 0.058 | 0.100 | 0.119 | 0.070 | 0.149 |
| 0.121 | 0.096 | 0.160 | 0.106 | 0.042 | 0.066 | 0.192 |
| 0.121 | 0.080 | 0.057 | 0.103 | 0.141 | 0.063 | 0.106 |
| 0.121 | 0.053 | 0.056 | 0.103 | 0.164 | 0.063 | 0.166 |
| 0.121 | 0.114 | 0.057 | 0.118 | 0.051 | 0.049 | 0.116 |
| 0.122 | 0.109 | 0.136 | 0.096 | 0.173 | 0.057 | 0.122 |
| 0.122 | 0.021 | 0.176 | 0.076 | 0.066 | 0.054 | 0.124 |
| 0.122 | 0.150 | 0.050 | 0.108 | 0.054 | 0.056 | 0.122 |
| 0.125 | 0.133 | 0.034 | 0.138 | 0.068 | 0.070 | 0.109 |
| 0.139 | 0.167 | 0.071 | 0.119 | 0.090 | 0.060 | 0.092 |
| 0.145 | 0.129 | 0.117 | 0.119 | 0.090 | 0.073 | 0.160 |
| 0.145 | 0.144 | 0.061 | 0.062 | 0.050 | 0.067 | 0.131 |
| 0.146 | 0.141 | 0.065 | 0.037 | 0.160 | 0.052 | 0.100 |
| 0.146 | 0.155 | 0.024 | 0.056 | 0.046 | 0.071 | 0.187 |
| 0.146 | 0.167 | 0.028 | 0.112 | 0.040 | 0.037 | 0.055 |
| 0.146 | 0.137 | 0.038 | 0.105 | 0.120 | 0.027 | 0.057 |
| 0.147 | 0.120 | 0.082 | 0.058 | 0.055 | 0.034 | 0.194 |
| 0.148 | 0.178 | 0.159 | 0.114 | 0.033 | 0.167 | 0.169 |
| 0.148 | 0.186 | 0.230 | 0.140 | 0.033 | 0.175 | 0.198 |
| 0.148 | 0.112 | 0.069 | 0.142 | 0.074 | 0.174 | 0.176 |
| 0.148 | 0.113 | 0.112 | 0.101 | 0.140 | 0.170 | 0.206 |
| 0.148 | 0.161 | 0.097 | 0.098 | 0.064 | 0.048 | 0.202 |
| 0.148 | 0.193 | 0.279 | 0.154 | 0.194 | 0.085 | 0.189 |
| 0.149 | 0.125 | 0.080 | 0.045 | 0.123 | 0.091 | 0.163 |
| 0.149 | 0.161 | 0.189 | 0.181 | 0.249 | 0.061 | 0.168 |

| | | | | | | |
|---|---|---|---|---|---|---|
| 0.149 | 0.191 | 0.300 | 0.031 | 0.222 | 0.165 | 0.186 |
| 0.149 | 0.220 | 0.195 | 0.174 | 0.084 | 0.160 | 0.159 |
| 0.149 | 0.227 | 0.177 | 0.188 | 0.091 | 0.166 | 0.182 |
| 0.150 | 0.113 | 0.155 | 0.184 | 0.071 | 0.183 | 0.166 |
| 0.153 | 0.183 | 0.262 | 0.049 | 0.114 | 0.163 | 0.149 |
| 0.164 | 0.134 | 0.118 | 0.064 | 0.122 | 0.269 | 0.210 |
| 0.170 | 0.246 | 0.199 | 0.157 | 0.166 | 0.274 | 0.193 |
| 0.174 | 0.217 | 0.117 | 0.192 | 0.065 | 0.167 | 0.198 |
| 0.174 | 0.159 | 0.178 | 0.166 | 0.085 | 0.144 | 0.232 |
| 0.175 | 0.157 | 0.270 | 0.114 | 0.060 | 0.169 | 0.237 |
| 0.176 | 0.179 | 0.283 | 0.067 | 0.142 | 0.165 | 0.202 |
| 0.176 | 0.147 | 0.184 | 0.056 | 0.041 | 0.203 | 0.237 |
| 0.176 | 0.160 | 0.165 | 0.055 | 0.178 | 0.232 | 0.229 |
| 0.176 | 0.170 | 0.221 | 0.110 | 0.240 | 0.251 | 0.227 |
| 0.176 | 0.208 | 0.152 | 0.179 | 0.198 | 0.263 | 0.251 |
| 0.176 | 0.249 | 0.150 | 0.170 | 0.230 | 0.266 | 0.261 |
| 0.176 | 0.173 | 0.178 | 0.164 | 0.231 | 0.190 | 0.197 |
| 0.176 | 0.316 | 0.159 | 0.202 | 0.265 | 0.268 | 0.225 |
| 0.177 | 0.226 | 0.154 | 0.207 | 0.241 | 0.267 | 0.214 |
| 0.177 | 0.258 | 0.224 | 0.220 | 0.279 | 0.163 | 0.235 |
| 0.177 | 0.225 | 0.292 | 0.273 | 0.236 | 0.187 | 0.213 |
| 0.177 | 0.145 | 0.176 | 0.187 | 0.256 | 0.268 | 0.199 |
| 0.178 | 0.187 | 0.193 | 0.183 | 0.228 | 0.263 | 0.213 |
| 0.178 | 0.112 | 0.274 | 0.190 | 0.238 | 0.284 | 0.205 |
| 0.178 | 0.136 | 0.219 | 0.226 | 0.194 | 0.271 | 0.288 |
| 0.187 | 0.196 | 0.246 | 0.181 | 0.185 | 0.170 | 0.218 |
| 0.193 | 0.172 | 0.182 | 0.179 | 0.195 | 0.173 | 0.162 |

**Table 7** Velocity at Outlet for different Models for Fr = 1.85

| | **Velocity at Outlet (m/s) Fr = 1.85** | | | | | |
|---|---|---|---|---|---|---|
| **$Y_{outlet}$ (m)** | **M-I** | **M-II** | **M-III** | **M-IV** | **M-V** | **M-VI** |
| 0.117 | 1.528 | 0.000 | 1.203 | 1.260 | 1.156 | 1.594 |
| 0.117 | 0.000 | 0.000 | 0.000 | 1.143 | 1.135 | 0.000 |
| 0.118 | 0.000 | 1.395 | 0.000 | 1.123 | 0.000 | 0.000 |
| 0.118 | 1.453 | 1.372 | 1.205 | 0.000 | 0.000 | 1.539 |
| 0.119 | 1.479 | 1.071 | 1.206 | 0.000 | 1.108 | 1.668 |
| 0.120 | 1.452 | 1.075 | 1.235 | 1.160 | 1.162 | 1.705 |
| 0.120 | 1.439 | 1.211 | 1.201 | 1.160 | 1.232 | 1.734 |
| 0.120 | 1.431 | 1.444 | 1.121 | 1.225 | 1.063 | 1.725 |
| 0.120 | 1.438 | 1.382 | 1.124 | 1.148 | 0.999 | 1.685 |
| 0.120 | 1.466 | 1.377 | 1.107 | 1.194 | 1.077 | 1.727 |
| 0.120 | 1.433 | 1.394 | 1.105 | 1.102 | 1.254 | 1.697 |

| | | | | | | |
|---|---|---|---|---|---|---|
| 0.120 | 1.415 | 1.124 | 1.100 | 1.190 | 1.044 | 1.779 |
| 0.120 | 1.440 | 1.140 | 1.109 | 1.178 | 0.996 | 1.716 |
| 0.121 | 1.416 | 1.307 | 1.006 | 1.191 | 1.004 | 1.743 |
| 0.121 | 1.434 | 1.313 | 1.008 | 1.174 | 1.316 | 1.683 |
| 0.121 | 1.380 | 1.246 | 1.033 | 1.183 | 1.265 | 1.764 |
| 0.121 | 1.404 | 1.039 | 1.046 | 1.162 | 1.251 | 1.602 |
| 0.122 | 1.429 | 1.332 | 1.049 | 1.207 | 1.121 | 1.705 |
| 0.122 | 1.425 | 1.316 | 1.079 | 1.121 | 0.922 | 1.733 |
| 0.122 | 1.414 | 1.036 | 1.026 | 0.971 | 1.264 | 1.722 |
| 0.125 | 1.401 | 0.994 | 1.004 | 0.987 | 1.165 | 1.549 |
| 0.139 | 1.355 | 1.138 | 1.009 | 0.936 | 0.927 | 1.378 |
| 0.145 | 1.294 | 1.094 | 0.770 | 0.871 | 0.867 | 1.535 |
| 0.145 | 1.311 | 1.048 | 1.047 | 0.809 | 1.271 | 1.526 |
| 0.146 | 1.215 | 0.828 | 0.619 | 0.790 | 0.767 | 1.539 |
| 0.146 | 1.224 | 0.000 | 0.000 | 0.856 | 0.000 | 1.518 |
| 0.146 | 1.243 | 0.000 | 0.000 | 0.771 | 0.000 | 0.000 |
| 0.146 | 1.170 | 0.854 | 0.778 | 0.830 | 1.249 | 0.000 |
| 0.147 | 0.000 | 0.878 | 0.752 | 0.845 | 0.816 | 1.391 |
| 0.148 | 0.000 | 1.103 | 0.750 | 0.000 | 0.756 | 1.461 |
| 0.148 | 1.193 | 1.054 | 0.781 | 0.000 | 0.845 | 1.398 |
| 0.148 | 1.264 | 0.962 | 0.767 | 0.750 | 0.768 | 1.429 |
| 0.148 | 1.248 | 1.051 | 0.726 | 0.807 | 1.116 | 1.491 |
| 0.148 | 1.230 | 1.058 | 0.665 | 0.793 | 0.873 | 1.491 |
| 0.148 | 1.054 | 0.980 | 1.013 | 0.865 | 0.941 | 1.456 |
| 0.149 | 1.231 | 0.902 | 0.698 | 0.807 | 0.781 | 1.333 |
| 0.149 | 1.113 | 0.993 | 0.701 | 0.767 | 0.722 | 1.420 |
| 0.149 | 1.124 | 0.952 | 1.013 | 0.863 | 0.922 | 1.346 |
| 0.149 | 1.038 | 0.889 | 0.720 | 0.758 | 0.851 | 1.297 |
| 0.149 | 1.176 | 0.813 | 1.046 | 0.816 | 0.977 | 1.424 |
| 0.150 | 1.190 | 0.755 | 0.853 | 0.672 | 0.704 | 1.325 |
| 0.153 | 1.100 | 0.913 | 0.664 | 0.985 | 1.116 | 1.146 |
| 0.164 | 1.102 | 0.887 | 0.719 | 0.678 | 0.746 | 1.222 |
| 0.170 | 0.962 | 0.739 | 0.786 | 0.711 | 0.705 | 1.249 |
| 0.174 | 1.024 | 0.802 | 0.780 | 0.928 | 1.110 | 1.089 |
| 0.174 | 0.836 | 0.785 | 0.712 | 0.741 | 0.737 | 1.184 |
| 0.175 | 0.937 | 0.780 | 0.770 | 0.652 | 0.698 | 1.129 |
| 0.176 | 0.916 | 0.757 | 0.801 | 0.746 | 0.000 | 0.994 |
| 0.176 | 0.890 | 0.000 | 0.679 | 0.703 | 0.000 | 1.040 |
| 0.176 | 0.838 | 0.000 | 0.798 | 0.681 | 0.922 | 1.030 |
| 0.176 | 0.885 | 0.772 | 0.000 | 0.692 | 0.806 | 1.014 |
| 0.176 | 0.785 | 0.778 | 0.000 | 0.678 | 0.838 | 0.000 |
| 0.176 | 0.767 | 0.739 | 0.637 | 0.000 | 0.798 | 0.000 |
| 0.176 | 0.681 | 0.773 | 0.721 | 0.000 | 0.751 | 1.071 |
| 0.176 | 0.769 | 0.770 | 0.762 | 0.712 | 0.763 | 1.070 |
| 0.177 | 0.686 | 0.788 | 0.758 | 0.751 | 0.824 | 1.008 |

| | | | | | | |
|---|---|---|---|---|---|---|
| 0.177 | 0.563 | 0.779 | 0.769 | 0.682 | 0.748 | 1.108 |
| 0.177 | 0.682 | 0.759 | 0.768 | 0.693 | 0.771 | 1.133 |
| 0.177 | 0.650 | 0.766 | 0.761 | 0.707 | 0.680 | 1.036 |
| 0.178 | 0.600 | 0.769 | 0.752 | 0.720 | 0.809 | 1.002 |
| 0.178 | 0.634 | 0.765 | 0.728 | 0.807 | 0.728 | 0.894 |
| 0.178 | 0.469 | 0.728 | 0.773 | 0.714 | 0.768 | 1.002 |
| 0.187 | 0.607 | 0.732 | 0.687 | 0.787 | 0.734 | 0.927 |
| 0.193 | 0.620 | 0.784 | 0.653 | 0.717 | 0.885 | 0.808 |

**Table 8** Velocity at Outlet for different models for Fr = 2.85

| | **Velocity at Outlet (m/s) Fr = 2.85** | | | | | |
|---|---|---|---|---|---|---|
| **$Y_{outlet}$ (m)** | **M-I** | **M-II** | **M-III** | **M-IV** | **M-V** | **M-VI** |
| 0.113 | 1.678 | 0.000 | 0.000 | 1.470 | 1.526 | 1.762 |
| 0.117 | 0.000 | 0.000 | 0.000 | 1.480 | 1.575 | 0.000 |
| 0.117 | 0.000 | 1.475 | 0.000 | 1.485 | 0.000 | 0.000 |
| 0.118 | 1.561 | 1.482 | 1.462 | 0.000 | 0.000 | 1.689 |
| 0.118 | 1.554 | 1.247 | 1.419 | 0.000 | 1.436 | 1.827 |
| 0.119 | 1.603 | 1.255 | 1.316 | 1.535 | 1.649 | 1.859 |
| 0.120 | 1.457 | 1.376 | 1.242 | 1.370 | 1.437 | 1.907 |
| 0.120 | 1.527 | 1.595 | 1.380 | 1.447 | 1.507 | 1.840 |
| 0.120 | 1.564 | 1.491 | 1.471 | 1.559 | 1.405 | 1.768 |
| 0.120 | 1.496 | 1.566 | 1.482 | 1.281 | 1.414 | 1.835 |
| 0.120 | 1.489 | 1.501 | 1.278 | 1.332 | 1.493 | 1.807 |
| 0.120 | 1.499 | 1.303 | 1.430 | 1.498 | 1.376 | 1.854 |
| 0.121 | 1.596 | 1.295 | 1.294 | 1.471 | 1.313 | 1.923 |
| 0.121 | 1.457 | 1.521 | 1.361 | 1.351 | 1.331 | 1.866 |
| 0.121 | 1.489 | 1.381 | 1.377 | 1.534 | 1.543 | 1.842 |
| 0.121 | 1.460 | 1.316 | 1.364 | 1.423 | 1.467 | 1.875 |
| 0.122 | 1.570 | 1.259 | 1.251 | 1.374 | 1.531 | 1.744 |
| 0.122 | 1.520 | 1.498 | 1.384 | 1.488 | 1.377 | 1.867 |
| 0.122 | 1.560 | 1.497 | 1.236 | 1.374 | 1.320 | 1.933 |
| 0.123 | 1.483 | 1.336 | 1.335 | 1.353 | 1.610 | 1.858 |
| 0.131 | 1.562 | 1.390 | 1.293 | 1.377 | 1.501 | 1.714 |
| 0.139 | 1.461 | 1.243 | 1.421 | 1.301 | 1.445 | 1.472 |
| 0.143 | 1.459 | 1.179 | 1.076 | 1.355 | 1.359 | 1.702 |
| 0.145 | 1.492 | 1.170 | 1.047 | 1.141 | 1.249 | 1.572 |
| 0.146 | 1.339 | 0.958 | 0.842 | 1.301 | 1.237 | 1.573 |
| 0.146 | 1.371 | 0.000 | 0.000 | 1.094 | 0.000 | 1.583 |
| 0.146 | 1.304 | 0.000 | 0.000 | 0.956 | 0.000 | 0.000 |
| 0.146 | 1.192 | 0.987 | 1.200 | 1.353 | 1.266 | 0.000 |

| | | | | | | |
|---|---|---|---|---|---|---|
| 0.147 | 0.000 | 1.024 | 0.959 | 1.126 | 1.296 | 1.463 |
| 0.147 | 0.000 | 1.257 | 1.220 | 0.000 | 1.143 | 1.607 |
| 0.147 | 1.341 | 1.138 | 0.894 | 0.000 | 1.115 | 1.606 |
| 0.148 | 1.427 | 1.091 | 1.216 | 1.102 | 1.047 | 1.516 |
| 0.148 | 1.344 | 1.290 | 1.273 | 1.151 | 1.272 | 1.518 |
| 0.148 | 1.287 | 1.328 | 1.312 | 1.135 | 1.459 | 1.634 |
| 0.148 | 1.242 | 1.002 | 1.141 | 1.077 | 1.401 | 1.758 |
| 0.148 | 1.302 | 1.013 | 0.912 | 1.150 | 1.277 | 1.460 |
| 0.148 | 1.250 | 1.076 | 0.970 | 1.066 | 1.083 | 1.794 |
| 0.149 | 1.286 | 1.192 | 1.252 | 1.139 | 1.288 | 1.786 |
| 0.149 | 1.222 | 1.076 | 1.108 | 1.096 | 1.274 | 1.428 |
| 0.149 | 1.266 | 0.964 | 1.361 | 0.996 | 1.259 | 1.509 |
| 0.153 | 1.301 | 1.000 | 1.136 | 0.863 | 1.153 | 1.840 |
| 0.154 | 1.119 | 0.946 | 1.087 | 1.124 | 1.088 | 1.201 |
| 0.164 | 1.208 | 0.907 | 0.883 | 0.850 | 1.377 | 1.252 |
| 0.165 | 1.101 | 0.735 | 1.006 | 1.079 | 1.070 | 1.160 |
| 0.171 | 1.195 | 0.788 | 0.947 | 0.877 | 0.955 | 1.087 |
| 0.173 | 0.980 | 0.750 | 0.708 | 0.862 | 1.010 | 1.014 |
| 0.174 | 1.115 | 0.796 | 0.926 | 0.696 | 1.230 | 1.084 |
| 0.175 | 0.965 | 0.711 | 1.050 | 1.066 | 0.000 | 1.045 |
| 0.175 | 1.043 | 0.000 | 0.669 | 0.765 | 0.000 | 1.114 |
| 0.176 | 0.958 | 0.000 | 1.145 | 0.780 | 0.947 | 1.025 |
| 0.176 | 0.911 | 0.851 | 0.000 | 0.680 | 0.857 | 1.344 |
| 0.176 | 0.946 | 0.776 | 0.000 | 0.732 | 1.068 | 0.000 |
| 0.176 | 0.779 | 0.725 | 0.661 | 0.000 | 1.019 | 0.000 |
| 0.176 | 0.790 | 0.915 | 0.690 | 0.000 | 0.907 | 1.622 |
| 0.176 | 0.904 | 0.913 | 0.908 | 0.774 | 0.908 | 1.074 |
| 0.176 | 0.790 | 0.914 | 1.058 | 0.871 | 0.870 | 1.032 |
| 0.176 | 0.685 | 0.747 | 0.710 | 0.745 | 1.135 | 1.171 |
| 0.177 | 0.708 | 0.719 | 0.645 | 0.770 | 0.999 | 1.455 |
| 0.177 | 0.745 | 0.705 | 0.628 | 0.685 | 1.102 | 1.700 |
| 0.178 | 0.690 | 0.798 | 0.726 | 0.641 | 0.892 | 1.596 |
| 0.178 | 0.729 | 0.733 | 0.683 | 0.801 | 0.975 | 0.906 |
| 0.185 | 0.594 | 0.659 | 0.558 | 0.777 | 0.794 | 0.954 |
| 0.187 | 0.702 | 0.619 | 0.563 | 0.624 | 0.954 | 1.632 |
| 0.193 | 0.690 | 0.680 | 0.480 | 0.585 | 0.724 | 0.758 |

**Table 9** Velocity at Outlet for different models for Fr = 3.85

| | Velocity at Outlet (m/s) Fr = 3.85 | | | | | |
|---|---|---|---|---|---|---|
| $Y_{outlet}$ (m) | M-I | M-II | M-III | M-IV | M-V | M-VI |
| 0.117 | 1.796 | 0.000 | 1.534 | 1.728 | 1.685 | 1.922 |
| 0.117 | 0.000 | 0.000 | 0.000 | 1.736 | 1.684 | 0.000 |
| 0.118 | 0.000 | 1.717 | 0.000 | 1.718 | 0.000 | 0.000 |
| 0.118 | 1.716 | 1.535 | 1.662 | 0.000 | 0.000 | 1.810 |
| 0.119 | 1.647 | 1.570 | 1.587 | 0.000 | 1.605 | 1.913 |
| 0.120 | 1.728 | 1.526 | 1.433 | 1.718 | 1.766 | 2.040 |
| 0.120 | 1.453 | 1.387 | 1.680 | 1.642 | 1.701 | 2.095 |
| 0.120 | 1.566 | 1.705 | 1.491 | 1.740 | 1.669 | 2.091 |
| 0.120 | 1.675 | 1.719 | 1.698 | 1.739 | 1.568 | 1.985 |
| 0.120 | 1.517 | 1.688 | 1.032 | 1.664 | 1.599 | 2.075 |
| 0.120 | 1.521 | 1.726 | 1.445 | 1.625 | 1.705 | 2.011 |
| 0.120 | 1.572 | 1.460 | 1.690 | 1.634 | 1.575 | 2.133 |
| 0.120 | 1.702 | 1.486 | 1.539 | 1.556 | 1.511 | 2.154 |
| 0.121 | 1.465 | 1.531 | 1.591 | 1.634 | 1.527 | 2.141 |
| 0.121 | 1.502 | 1.582 | 1.026 | 1.686 | 1.713 | 1.963 |
| 0.121 | 1.494 | 1.467 | 1.568 | 1.504 | 1.683 | 2.149 |
| 0.121 | 1.709 | 1.461 | 1.018 | 1.728 | 1.675 | 1.964 |
| 0.122 | 1.600 | 1.546 | 1.431 | 1.612 | 1.586 | 2.022 |
| 0.122 | 1.632 | 1.465 | 1.293 | 1.610 | 1.496 | 2.183 |
| 0.122 | 1.543 | 1.490 | 1.308 | 1.457 | 1.667 | 2.172 |
| 0.125 | 1.688 | 1.513 | 1.298 | 1.481 | 1.737 | 1.924 |
| 0.139 | 1.595 | 1.486 | 1.321 | 1.333 | 1.518 | 1.753 |
| 0.145 | 1.629 | 1.411 | 1.430 | 1.310 | 1.436 | 1.830 |
| 0.145 | 1.640 | 1.418 | 1.314 | 1.324 | 1.474 | 1.757 |
| 0.146 | 1.452 | 1.404 | 1.148 | 1.220 | 1.399 | 1.773 |
| 0.146 | 1.502 | 0.000 | 0.000 | 1.283 | 0.000 | 1.767 |
| 0.146 | 1.316 | 0.000 | 0.000 | 1.250 | 0.000 | 0.000 |
| 0.146 | 1.207 | 1.435 | 1.215 | 1.104 | 1.253 | 0.000 |
| 0.147 | 0.000 | 1.370 | 1.261 | 1.291 | 1.202 | 1.718 |
| 0.148 | 0.000 | 1.380 | 1.113 | 0.000 | 1.113 | 1.733 |
| 0.148 | 1.518 | 1.153 | 1.125 | 0.000 | 1.073 | 1.898 |
| 0.148 | 1.570 | 1.362 | 1.307 | 1.275 | 1.141 | 1.707 |
| 0.148 | 1.444 | 1.425 | 1.189 | 1.276 | 1.162 | 1.773 |
| 0.148 | 1.349 | 1.471 | 1.298 | 1.274 | 1.257 | 1.896 |
| 0.148 | 1.372 | 0.941 | 1.259 | 1.003 | 1.300 | 1.928 |
| 0.149 | 1.328 | 1.321 | 1.109 | 1.116 | 1.225 | 1.641 |
| 0.149 | 1.339 | 1.143 | 1.114 | 0.843 | 1.041 | 1.940 |
| 0.149 | 1.378 | 1.359 | 1.202 | 0.895 | 1.286 | 2.024 |

| | | | | | | |
|---|---|---|---|---|---|---|
| 0.149 | 1.379 | 1.329 | 1.125 | 1.095 | 1.293 | 1.642 |
| 0.149 | 1.331 | 1.268 | 1.203 | 1.108 | 1.130 | 1.652 |
| 0.150 | 1.403 | 1.280 | 0.802 | 1.155 | 1.100 | 2.008 |
| 0.153 | 1.120 | 0.901 | 0.903 | 1.009 | 1.162 | 1.473 |
| 0.164 | 1.256 | 1.239 | 0.809 | 1.143 | 1.270 | 1.410 |
| 0.170 | 1.276 | 1.081 | 0.908 | 0.827 | 1.140 | 1.364 |
| 0.174 | 1.362 | 1.162 | 0.787 | 1.081 | 1.083 | 1.528 |
| 0.174 | 1.141 | 0.914 | 0.818 | 1.097 | 1.069 | 1.293 |
| 0.175 | 1.291 | 0.782 | 0.909 | 1.044 | 1.152 | 1.303 |
| 0.176 | 0.985 | 0.678 | 0.904 | 1.079 | 0.000 | 1.215 |
| 0.176 | 1.215 | 0.000 | 0.775 | 1.018 | 0.000 | 1.347 |
| 0.176 | 1.094 | 0.000 | 0.635 | 0.836 | 0.844 | 1.195 |
| 0.176 | 0.959 | 0.896 | 0.000 | 1.056 | 0.867 | 1.636 |
| 0.176 | 1.082 | 1.016 | 0.000 | 1.040 | 1.028 | 0.000 |
| 0.176 | 0.813 | 0.972 | 0.888 | 0.000 | 1.073 | 0.000 |
| 0.176 | 0.945 | 0.985 | 0.864 | 0.000 | 1.076 | 1.789 |
| 0.176 | 1.057 | 0.968 | 0.921 | 0.927 | 0.950 | 1.191 |
| 0.177 | 0.895 | 1.013 | 1.011 | 0.909 | 0.931 | 1.185 |
| 0.177 | 0.816 | 1.080 | 1.010 | 0.719 | 1.076 | 1.457 |
| 0.177 | 0.750 | 0.907 | 0.902 | 0.662 | 1.070 | 1.715 |
| 0.177 | 0.858 | 0.908 | 0.905 | 0.879 | 1.048 | 1.831 |
| 0.178 | 0.776 | 0.955 | 0.857 | 0.896 | 0.995 | 1.830 |
| 0.178 | 0.830 | 0.993 | 0.850 | 0.842 | 0.951 | 1.070 |
| 0.178 | 0.721 | 0.723 | 0.720 | 0.663 | 0.953 | 1.047 |
| 0.187 | 0.789 | 0.598 | 0.555 | 0.902 | 0.906 | 1.810 |
| 0.193 | 0.788 | 0.813 | 0.774 | 0.903 | 0.905 | 0.969 |

**Table 10** Showing Kinetic Energy (K.E) and Specific Energy (Sp.E) Losses for **Fr =1.85**

| Model | $V_{inlet}$ (m/s) | $V_{outlet}$ (m/s) | $Y_{inlet}$ (m) | $Y_{outlet}$ (m) | $(K.E/Mass)_{inlet}$ (m) | $(K.E/Mass)_{outlet}$ (m) | $(Sp.E)_{inlet}$ (m) | $(Sp.E)_{outlet}$ (m) | ΔK.E (m) | ΔSp.E (m) |
|---|---|---|---|---|---|---|---|---|---|---|
| M-I | 1.767 | 0.989 | 0.093 | 0.072 | 0.159 | 0.050 | 0.252 | 0.121 | 0.109 | 0.131 |
| M-II | 1.767 | 0.895 | 0.093 | 0.051 | 0.159 | 0.041 | 0.252 | 0.092 | 0.118 | 0.160 |
| M-III | 1.767 | 0.799 | 0.093 | 0.044 | 0.159 | 0.033 | 0.252 | 0.077 | 0.127 | 0.175 |
| M-IV | 1.767 | 0.812 | 0.093 | 0.047 | 0.159 | 0.034 | 0.252 | 0.081 | 0.126 | 0.171 |
| M-V | 1.767 | 0.853 | 0.093 | 0.051 | 0.159 | 0.037 | 0.252 | 0.088 | 0.122 | 0.164 |
| M-VI | 1.767 | 1.250 | 0.093 | 0.084 | 0.159 | 0.080 | 0.252 | 0.163 | 0.080 | 0.089 |

**Table 11** Showing Kinetic Energy (K.E) and Specific Energy (Sp.E) Losses for **Fr =2.85**

| Model | $V_{inlet}$ (m/s) | $V_{outlet}$ (m/s) | $Y_{inlet}$ (m) | $Y_{outlet}$ (m) | $(K.E/Mass)_{inlet}$ (m) | $(K.E/Mass)_{outlet}$ (m) | $(Sp.E)_{inlet}$ (m) | $(Sp.E)_{outlet}$ (m) | ΔK.E (m) | ΔSp.E (m) |
|---|---|---|---|---|---|---|---|---|---|---|
| M-I | 2.722 | 1.089 | 0.093 | 0.067 | 0.378 | 0.060 | 0.471 | 0.128 | 0.317 | 0.343 |
| M-II | 2.722 | 0.987 | 0.093 | 0.049 | 0.378 | 0.050 | 0.471 | 0.099 | 0.328 | 0.372 |
| M-III | 2.722 | 0.960 | 0.093 | 0.039 | 0.378 | 0.047 | 0.471 | 0.086 | 0.331 | 0.385 |
| M-IV | 2.722 | 1.006 | 0.093 | 0.046 | 0.378 | 0.052 | 0.471 | 0.097 | 0.326 | 0.373 |
| M-V | 2.722 | 1.114 | 0.093 | 0.047 | 0.378 | 0.063 | 0.471 | 0.110 | 0.314 | 0.360 |
| M-VI | 2.722 | 1.388 | 0.093 | 0.084 | 0.378 | 0.098 | 0.471 | 0.183 | 0.279 | 0.288 |

**Table 12 Showing** Kinetic Energy (K.E) and Specific Energy (Sp.E) Losses for **Fr =3.85**

| Model | $V_{inlet}$ (m/s) | $V_{outlet}$ (m/s) | $Y_{inlet}$ (m) | $Y_{outlet}$ (m) | $(K.E/Mass)_{inlet}$ (m) | $(K.E/Mass)_{outlet}$ (m) | $(Sp.E)_{inlet}$ (m) | $(Sp.E)_{outlet}$ (m) | ΔK.E (m) | ΔSp.E (m) |
|---|---|---|---|---|---|---|---|---|---|---|
| M-I | 3.677 | 1.180 | 0.093 | 0.068 | 0.689 | 0.071 | 0.782 | 0.139 | 0.618 | 0.643 |
| M-II | 3.677 | 1.142 | 0.093 | 0.058 | 0.689 | 0.067 | 0.782 | 0.124 | 0.623 | 0.658 |
| M-III | 3.677 | 1.040 | 0.093 | 0.047 | 0.689 | 0.055 | 0.782 | 0.102 | 0.634 | 0.680 |
| M-IV | 3.677 | 1.123 | 0.093 | 0.055 | 0.689 | 0.064 | 0.782 | 0.119 | 0.625 | 0.663 |
| M-V | 3.677 | 1.174 | 0.093 | 0.057 | 0.689 | 0.070 | 0.782 | 0.127 | 0.619 | 0.655 |
| M-VI | 3.677 | 1.567 | 0.093 | 0.085 | 0.689 | 0.125 | 0.782 | 0.210 | 0.564 | 0.572 |

**Table 13** Shear Stress at Bottom outlet for different Models for Fr = 1.85

| | **Wall Shear Stress at Outlet Bottom (Pa) Fr = 1.85** | | | | | |
|---|---|---|---|---|---|---|
| **$Y_{outlet}$ (m)** | **M-I** | **M-II** | **M-III** | **M-IV** | **M-V** | **M-VI** |
| 0.093 | 4.91 | 3.22 | 3.94 | 5.20 | 4.98 | 10.16 |
| 0.093 | 4.81 | 3.61 | 4.45 | 4.47 | 5.56 | 9.36 |
| 0.093 | 4.49 | 4.66 | 5.37 | 5.44 | 4.66 | 8.65 |
| 0.093 | 4.00 | 5.45 | 4.94 | 5.43 | 5.82 | 8.93 |
| 0.093 | 5.35 | 6.17 | 6.36 | 5.40 | 5.84 | 9.38 |
| 0.093 | 5.64 | 6.57 | 5.50 | 5.98 | 6.03 | 9.82 |
| 0.093 | 6.09 | 6.30 | 6.51 | 6.83 | 7.03 | 9.94 |
| 0.093 | 6.04 | 6.24 | 5.30 | 6.71 | 7.53 | 11.02 |

| | | | | | | |
|---|---|---|---|---|---|---|
| 0.093 | 5.87 | 5.67 | 4.97 | 7.05 | 7.04 | 11.75 |
| 0.093 | 5.88 | 5.10 | 5.71 | 7.42 | 7.10 | 12.00 |
| 0.093 | 5.90 | 5.94 | 4.73 | 7.07 | 7.10 | 12.35 |
| 0.093 | 5.32 | 6.59 | 5.83 | 6.64 | 6.84 | 12.73 |
| 0.093 | 5.53 | 6.71 | 4.85 | 6.10 | 5.90 | 11.72 |
| 0.093 | 7.14 | 7.07 | 5.87 | 5.54 | 5.52 | 11.08 |
| 0.093 | 5.85 | 6.96 | 4.81 | 5.21 | 5.25 | 12.09 |
| 0.093 | 5.89 | 5.87 | 6.17 | 4.89 | 5.27 | 10.76 |
| 0.093 | 6.06 | 4.97 | 6.43 | 4.79 | 5.19 | 10.79 |
| 0.093 | 5.64 | 5.10 | 7.03 | 4.71 | 5.34 | 9.80 |
| 0.093 | 5.77 | 5.61 | 5.97 | 3.98 | 4.90 | 8.48 |
| 0.093 | 5.42 | 4.10 | 5.79 | 3.48 | 4.07 | 7.38 |
| 0.093 | 6.12 | 3.57 | 3.42 | 3.67 | 3.84 | 7.83 |

**Table 14** Shear Stress at Bottom outlet for different Models for Fr = 2.85

| | **Wall Shear Stress at Outlet Bottom (Pa) Fr = 2.85** | | | | | |
|---|---|---|---|---|---|---|
| **$Y_{outlet}$ (m)** | **M-I** | **M-II** | **M-III** | **M-IV** | **M-V** | **M-VI** |
| 0.093 | 4.895 | 4.238 | 4.240 | 6.807 | 5.340 | 11.626 |
| 0.093 | 4.944 | 4.385 | 4.265 | 5.720 | 5.812 | 10.404 |
| 0.093 | 4.455 | 4.598 | 4.070 | 7.869 | 6.106 | 10.820 |
| 0.093 | 4.168 | 4.838 | 4.131 | 6.992 | 6.724 | 10.948 |
| 0.093 | 5.486 | 5.460 | 5.324 | 6.802 | 6.884 | 11.967 |
| 0.093 | 5.976 | 5.344 | 5.748 | 6.691 | 6.601 | 12.712 |
| 0.093 | 6.816 | 5.918 | 5.386 | 7.111 | 5.625 | 13.493 |
| 0.093 | 6.944 | 6.345 | 5.575 | 7.150 | 5.430 | 15.344 |
| 0.093 | 6.900 | 6.850 | 5.333 | 6.745 | 6.551 | 14.857 |
| 0.093 | 6.798 | 6.510 | 6.090 | 6.994 | 7.199 | 12.046 |
| 0.093 | 6.712 | 7.276 | 6.595 | 7.068 | 7.304 | 11.580 |
| 0.093 | 6.200 | 5.800 | 5.310 | 6.881 | 6.253 | 14.186 |
| 0.093 | 6.483 | 5.573 | 5.480 | 6.693 | 6.091 | 13.842 |
| 0.093 | 7.418 | 5.861 | 5.595 | 6.228 | 6.417 | 12.618 |
| 0.093 | 6.820 | 6.767 | 5.218 | 6.140 | 6.628 | 12.997 |
| 0.093 | 6.850 | 6.487 | 6.512 | 6.297 | 8.006 | 11.060 |
| 0.093 | 7.035 | 5.834 | 5.710 | 6.134 | 6.993 | 10.698 |
| 0.093 | 5.906 | 6.104 | 7.148 | 5.792 | 7.895 | 10.326 |
| 0.093 | 6.269 | 6.651 | 6.141 | 5.160 | 7.311 | 8.879 |
| 0.093 | 5.939 | 5.590 | 6.060 | 4.428 | 6.074 | 7.987 |
| 0.093 | 7.039 | 5.455 | 5.887 | 4.585 | 5.872 | 8.541 |

**Table 15** Shear Stress at Bottom outlet for different Models for Fr = 3.85

| | Wall Shear Stress at Outlet Bottom (Pa) Fr = 3.85 | | | | | |
|---|---|---|---|---|---|---|
| $Y_{outlet}$ (m) | M-I | M-II | M-III | M-IV | M-V | M-VI |
| 0.093 | 4.901 | 6.028 | 5.105 | 5.507 | 6.439 | 10.452 |
| 0.093 | 5.251 | 6.232 | 5.823 | 5.848 | 6.241 | 10.899 |
| 0.093 | 4.379 | 7.037 | 6.851 | 7.201 | 8.093 | 12.576 |
| 0.093 | 4.167 | 7.182 | 7.154 | 7.836 | 8.655 | 14.156 |
| 0.093 | 6.259 | 4.267 | 4.429 | 4.999 | 5.487 | 15.575 |
| 0.093 | 7.064 | 3.859 | 3.374 | 7.269 | 8.116 | 16.449 |
| 0.093 | 7.812 | 4.658 | 4.371 | 7.750 | 8.639 | 18.012 |
| 0.093 | 7.860 | 8.083 | 8.342 | 8.834 | 9.107 | 18.343 |
| 0.093 | 7.807 | 8.361 | 8.628 | 9.608 | 8.510 | 18.113 |
| 0.093 | 7.725 | 8.775 | 8.353 | 9.797 | 8.580 | 17.518 |
| 0.093 | 7.794 | 7.852 | 7.602 | 9.325 | 9.188 | 15.445 |
| 0.093 | 7.500 | 7.796 | 7.721 | 8.353 | 8.727 | 14.465 |
| 0.093 | 7.960 | 7.293 | 6.647 | 8.675 | 8.477 | 14.422 |
| 0.093 | 7.971 | 6.999 | 6.315 | 8.090 | 8.493 | 14.520 |
| 0.093 | 8.843 | 5.123 | 5.951 | 6.716 | 8.539 | 12.609 |
| 0.093 | 8.268 | 5.453 | 6.916 | 7.344 | 9.998 | 13.735 |
| 0.093 | 8.195 | 5.916 | 5.851 | 6.173 | 8.748 | 13.170 |
| 0.093 | 6.137 | 6.074 | 6.079 | 6.396 | 9.011 | 12.034 |
| 0.093 | 6.578 | 6.491 | 5.553 | 5.320 | 8.338 | 10.169 |
| 0.093 | 7.047 | 5.950 | 5.137 | 5.448 | 6.069 | 8.964 |
| 0.093 | 7.690 | 5.385 | 5.159 | 5.436 | 6.630 | 9.137 |

## 4.3 Stream Lines Plots

This section contains plot of stream lines from inlet after the analysis is complete by fluent software. Also the variation in stream lines plot as distance between Impact wall and inlet increases from 2d (18.6 cm) to 4d (37.2 cm), gap between impact wall and basin floor increases from 0.5d (4.65 cm) to 1.5d (13.95 cm).

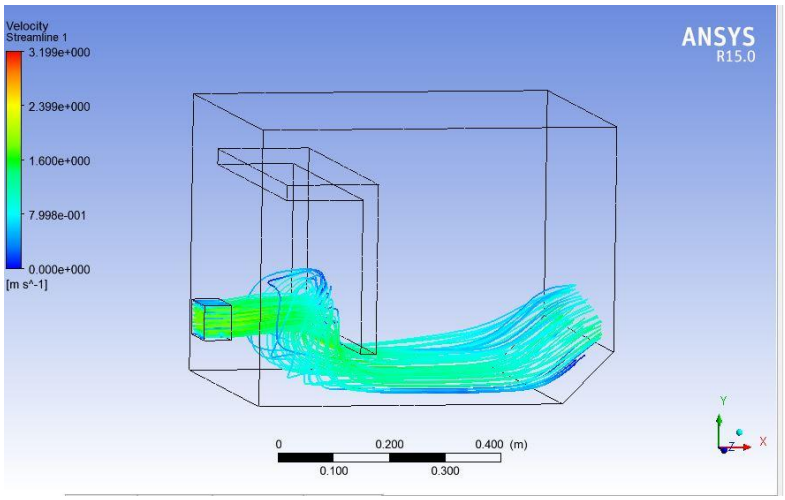


**Figure 15** Stream lines for M-I Fr 1.85

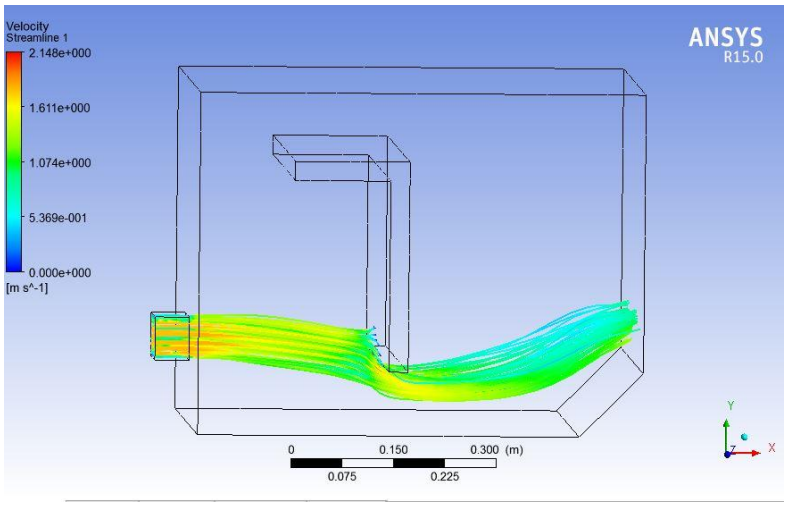


**Figure 16** Stream lines for M-II Fr 1.85

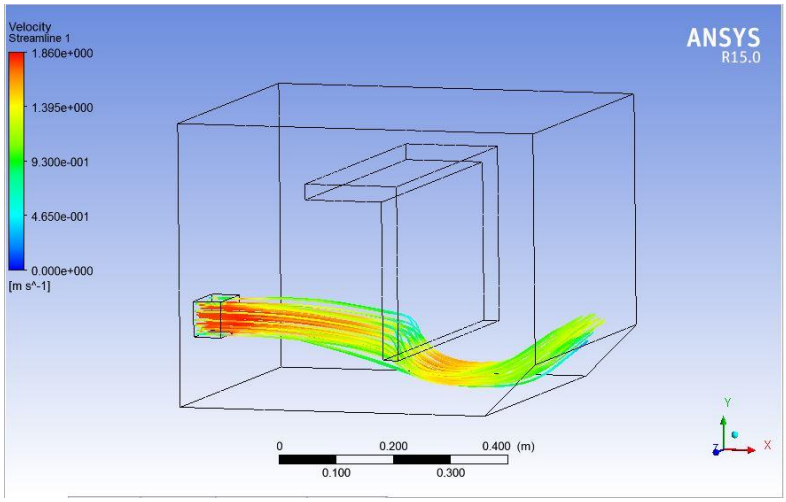


**Figure 17** Stream lines for M-III Fr 1.85

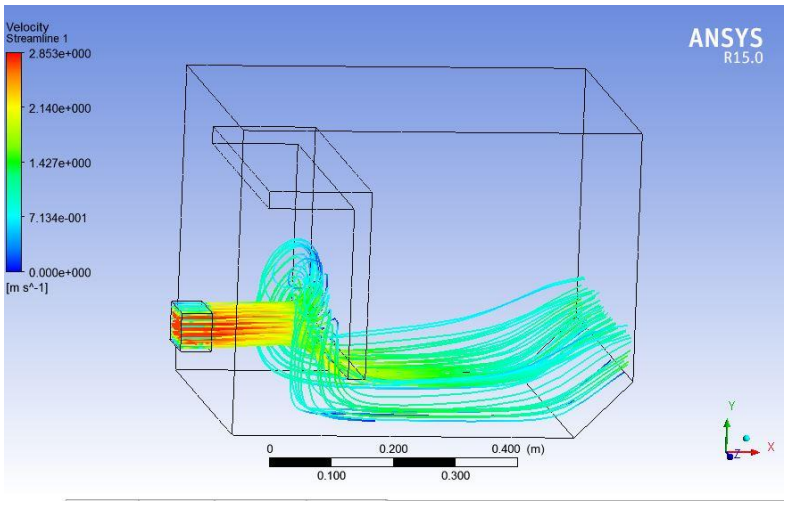


**Figure 18** Stream lines for M-I Fr 2.85

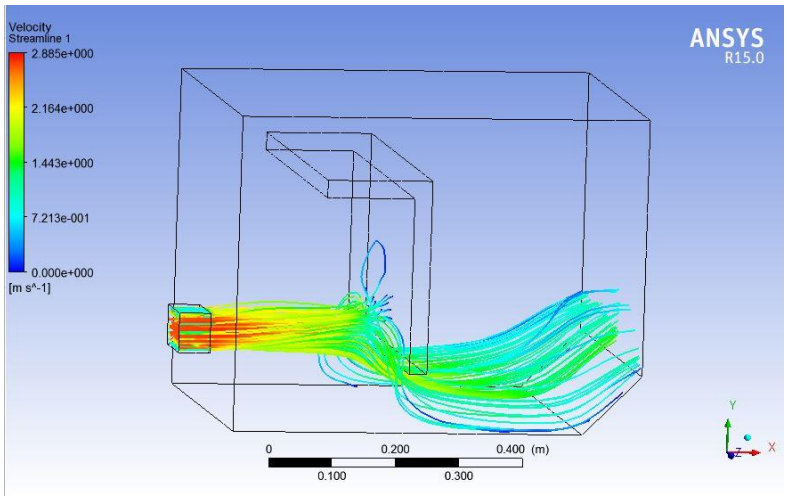


**Figure 19** Stream lines for M-II Fr 2.85

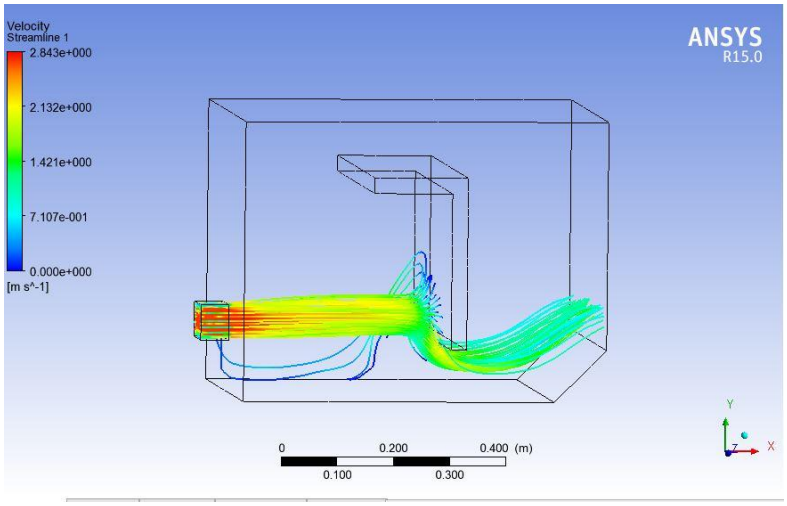


**Figure 20** Stream lines for M-III Fr 2.85

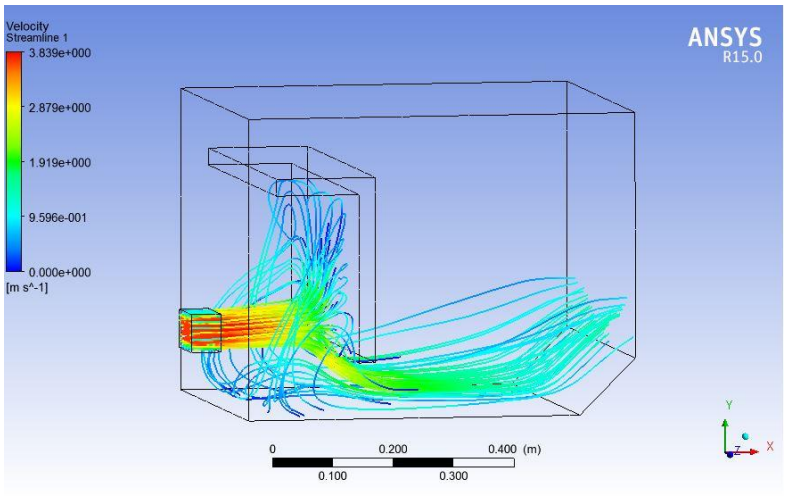


**Figure 21** Stream lines for M-I Fr 3.85

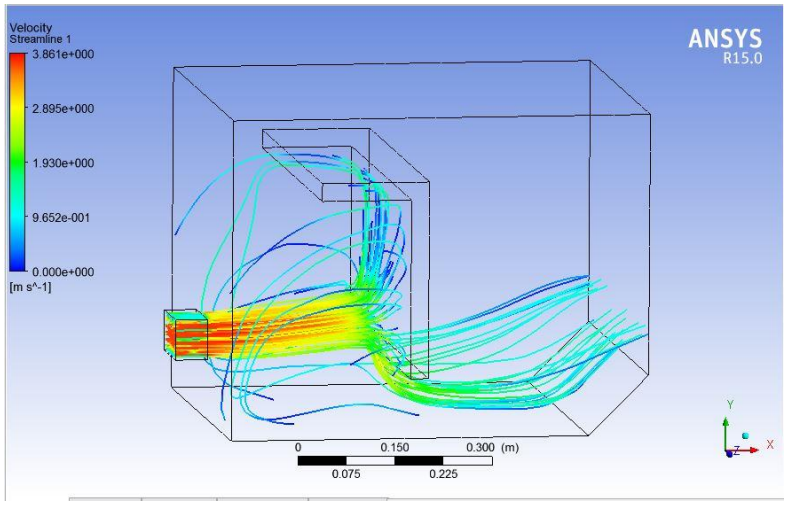


**Figure 22** Stream lines for M-II Fr 3.85

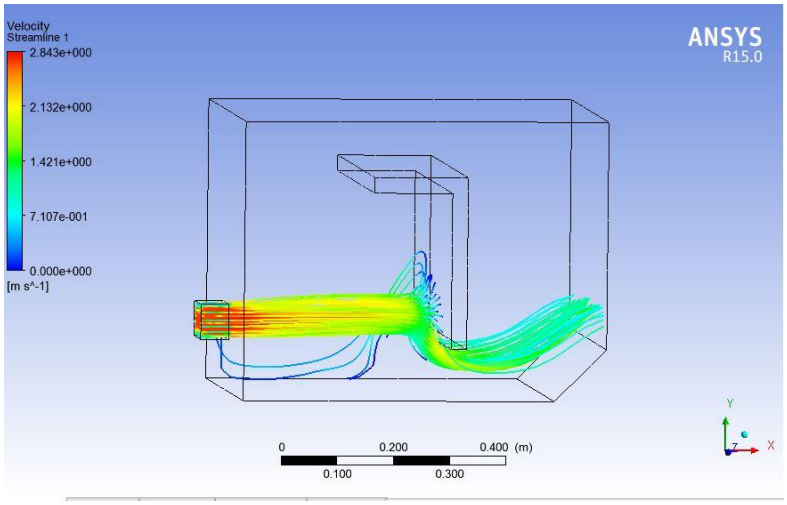


**Figure 23** Stream lines for M-III Fr 3.85

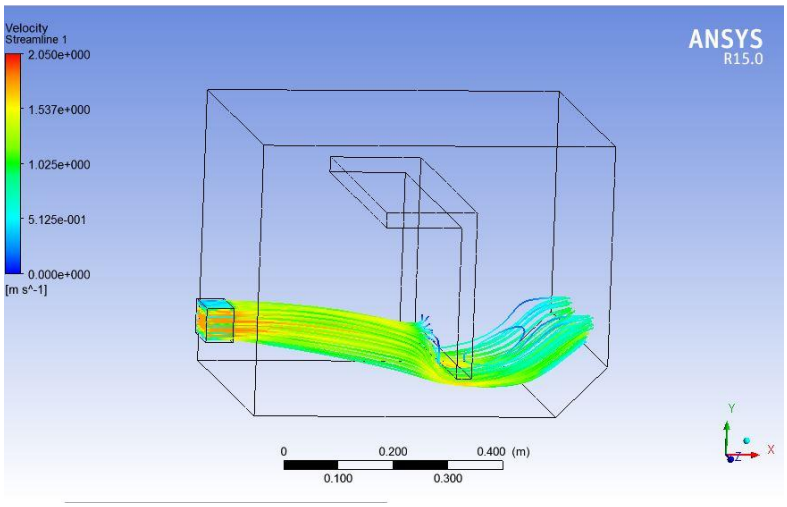


**Figure 24** Stream lines for M-IV Fr 1.85

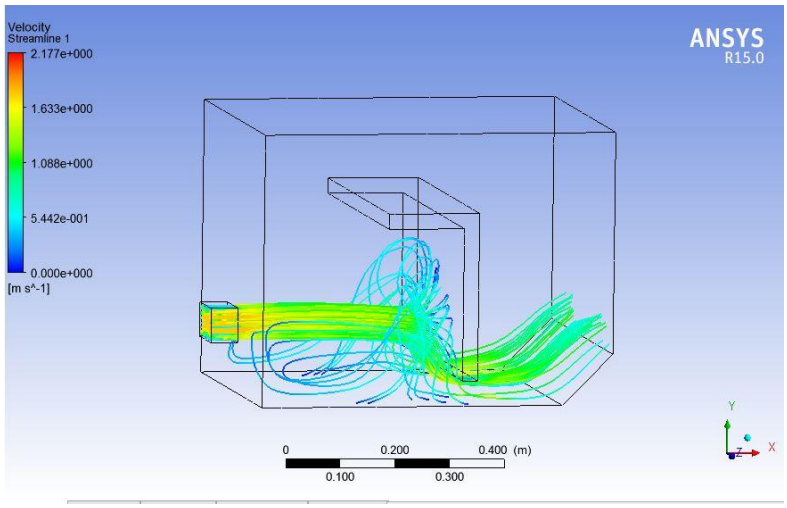


**Figure 25** Stream lines for M-V Fr 1.85

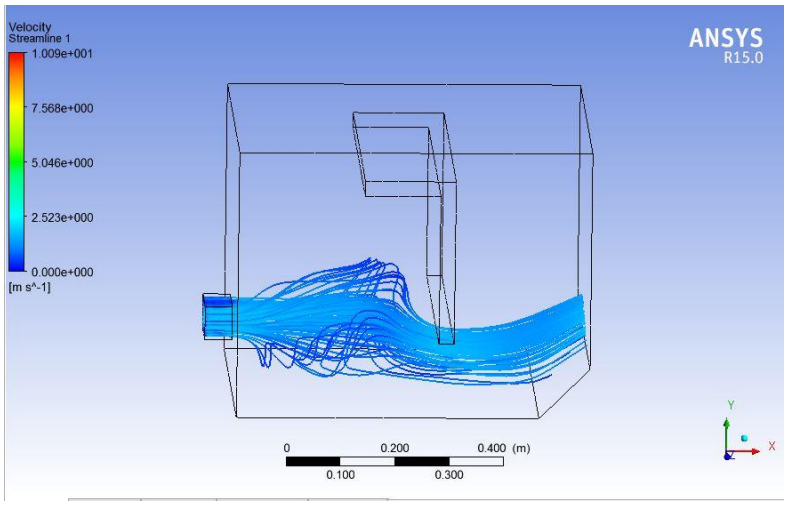


**Figure 26** Stream lines for M-VI Fr 1.85

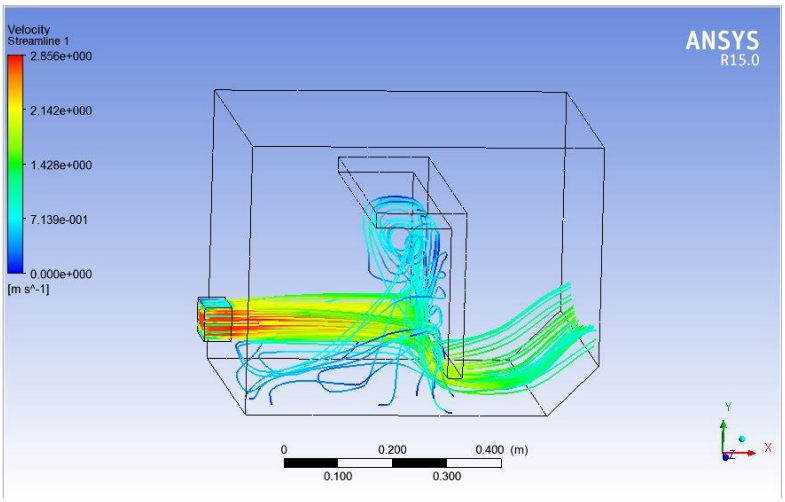


**Figure 27** Stream lines for M-IV Fr 2.85

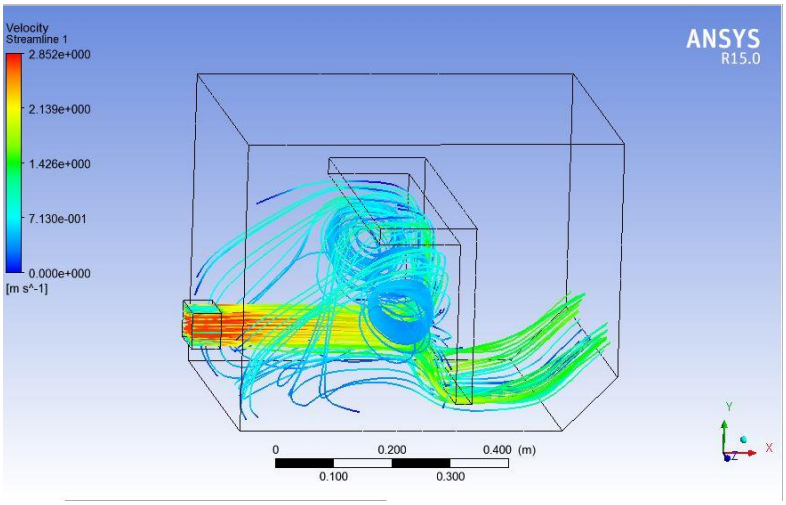


**Figure 28** Stream lines for M-V Fr 2.85

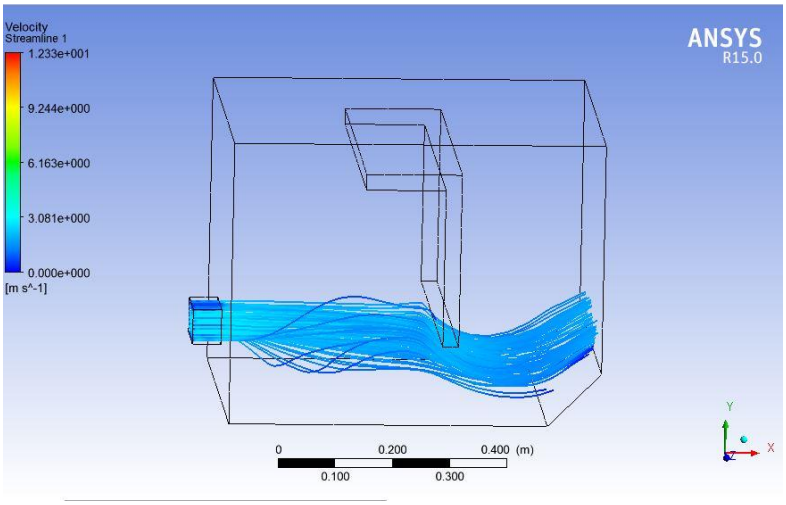


**Figure 29** Stream lines for M-VI Fr 2.85

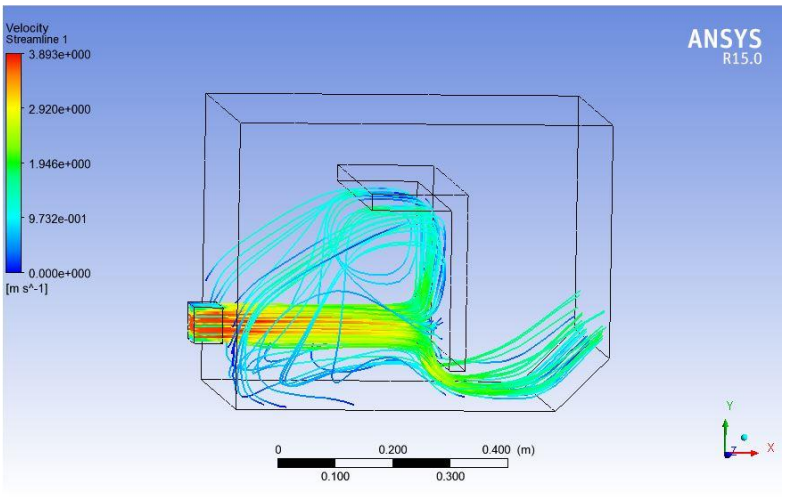


**Figure 30** Stream lines for M-IV Fr 3.85

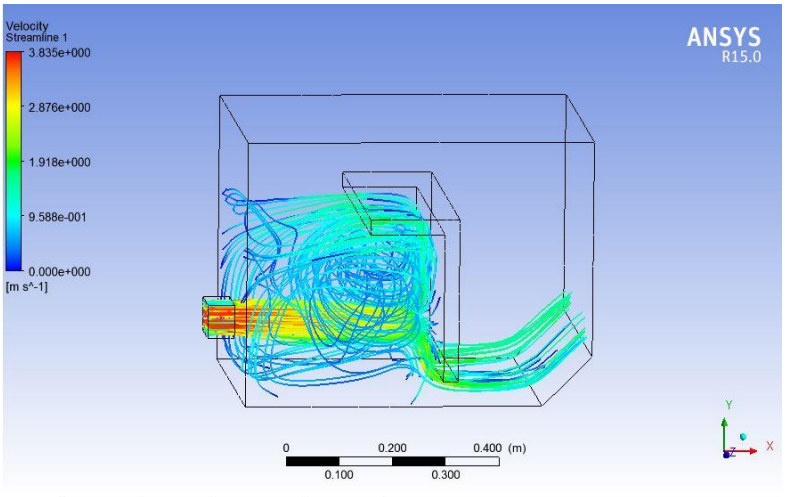


**Figure 31** Stream lines for M-V Fr 3.85

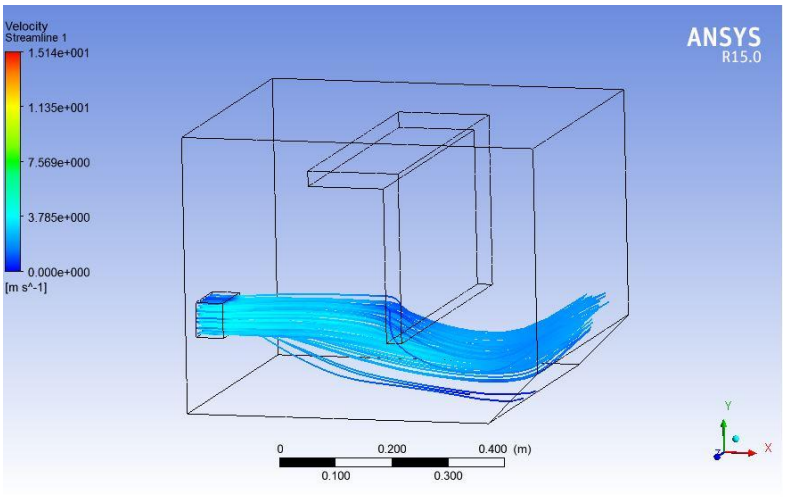


**Figure 32** Stream lines for M-VI Fr 3.85

# CHAPTER 5

# RESULTS AND DISCUSSIONS

## 5.1 Results

The results obtained from the analysis by fluent are presented in the form of Bar graphs comparing different models. The graphs are plotted for three different Froude Numbers i.e. 1.85, 2.85 and 3.85 for the following Parameters:

- Average, Maximum values of *Turbulent Kinetic Energy* for M-I, M-II and M-III model. Also another graph has been plotted between *Average Turbulent Kinetic Energy* and *Gap between Impact Wall and Basin Floor.*
- Average, Maximum values of *Velocity at Outlet* for M-I, M-II and M-III model. Also another graph has been plotted between *Average Velocity at Outlet* and *Gap between Impact Wall and Basin Floor.*
- Average, Maximum values of *Shear Stress at Bottom Outlet* for M-I, M-II & M-III model. Also another graph has been plotted between *Average Shear Stress at Bottom Outlet* and *Gap between Impact Wall and Basin Floor.*
- Kinetic Energy loss and Specific *Energy Losses* for M-I, M-II & M-III model. Also another graph has been plotted between *Energy Losses* and *Gap between Impact Wall and Basin Floor.*

*Turbulent Kinetic Energy Plot*

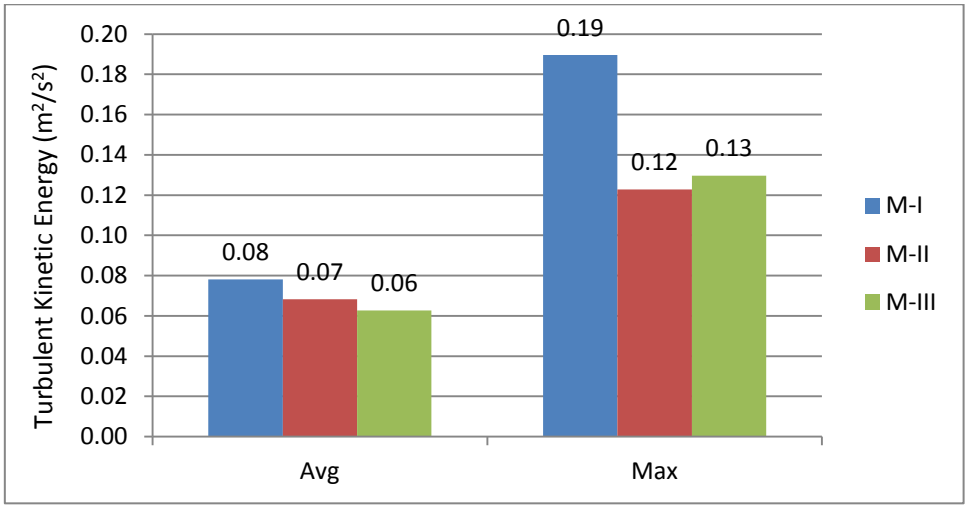


**Figure 33** Showing Turbulent Kinetic Energy for M-I M-II & M-III model for Fr =1.85

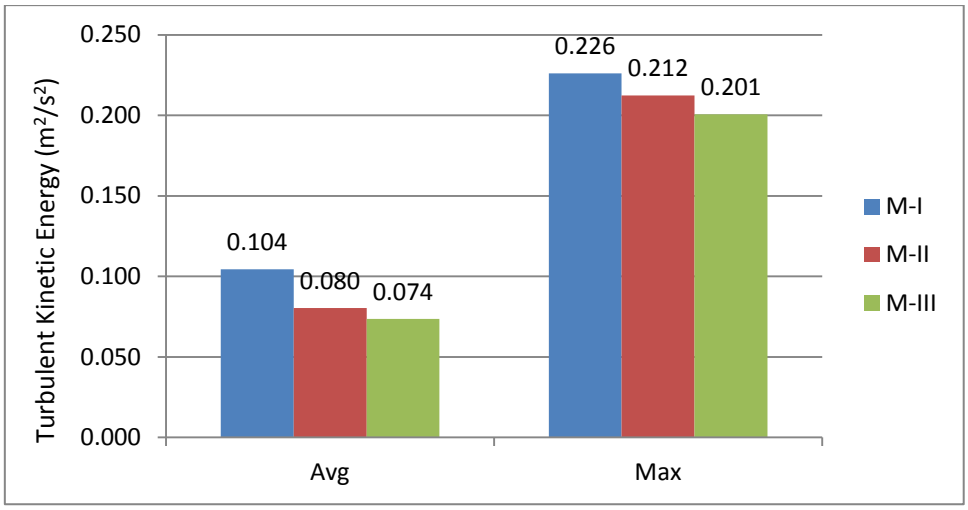


**Figure 34** Showing Turbulent Kinetic Energy for M-I M-II & M-III model for Fr =2.85

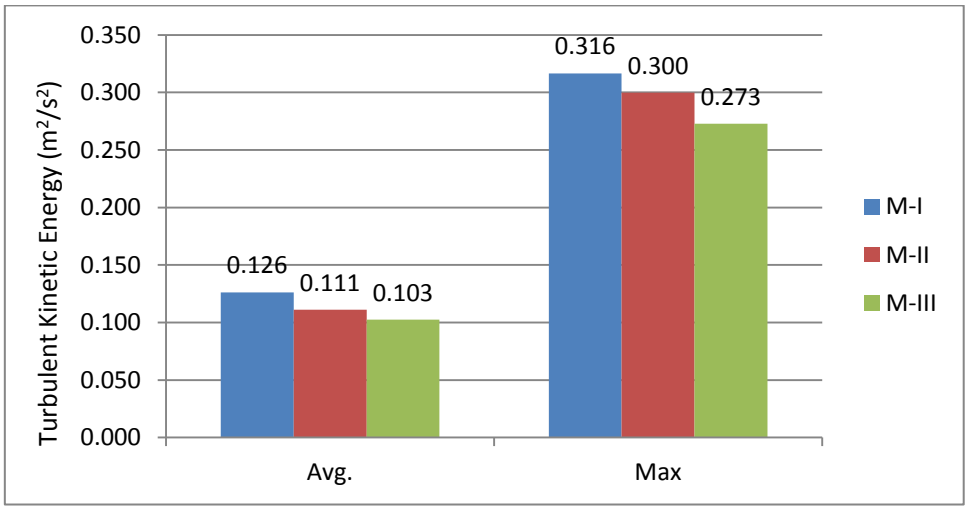


**Figure 35** Showing Turbulent Kinetic Energy for M-I M-II & M-III model for Fr =3.85

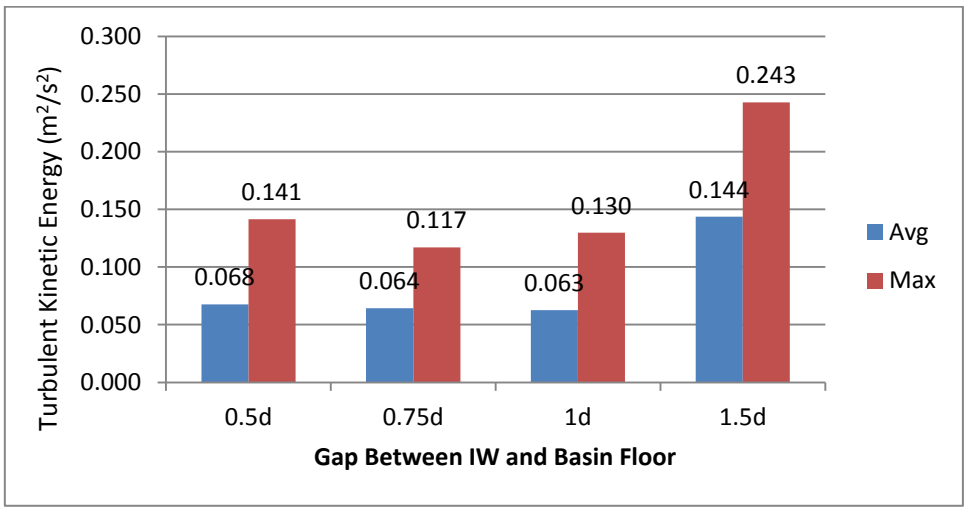


**Figure 36** Turbulent Kinetic Energy for M-III M-IV M-V M-VI model for Fr = 1.85

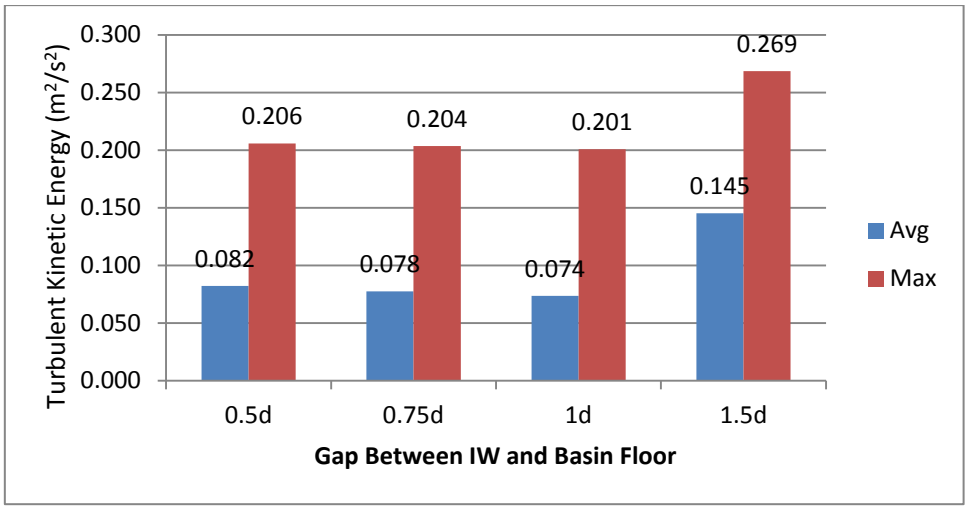


**Figure 37** Turbulent Kinetic Energy for M-III M-IV M-V M-VI model for Fr = 2.85

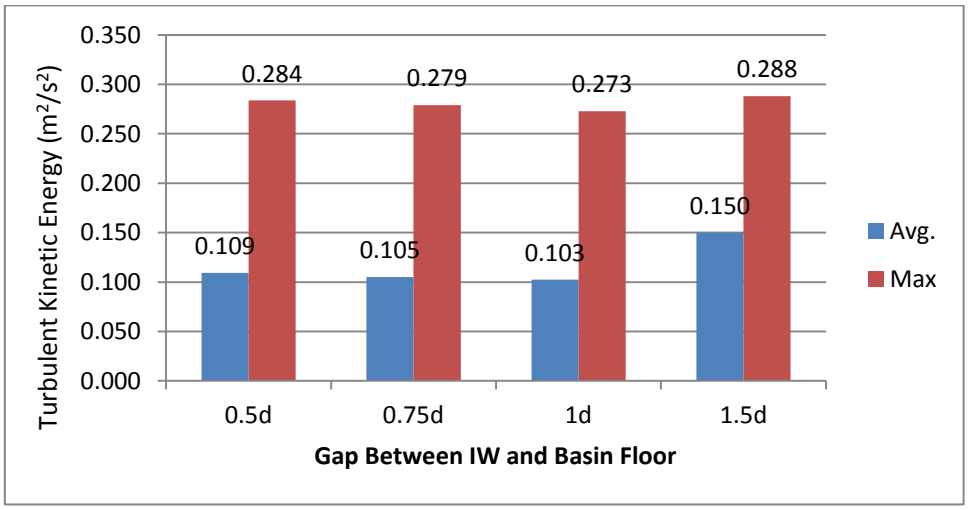


**Figure 38** Turbulent Kinetic Energy for M-III M-IV M-V M-VI model for Fr = 3.85

*Velocity at Outlet Plot*

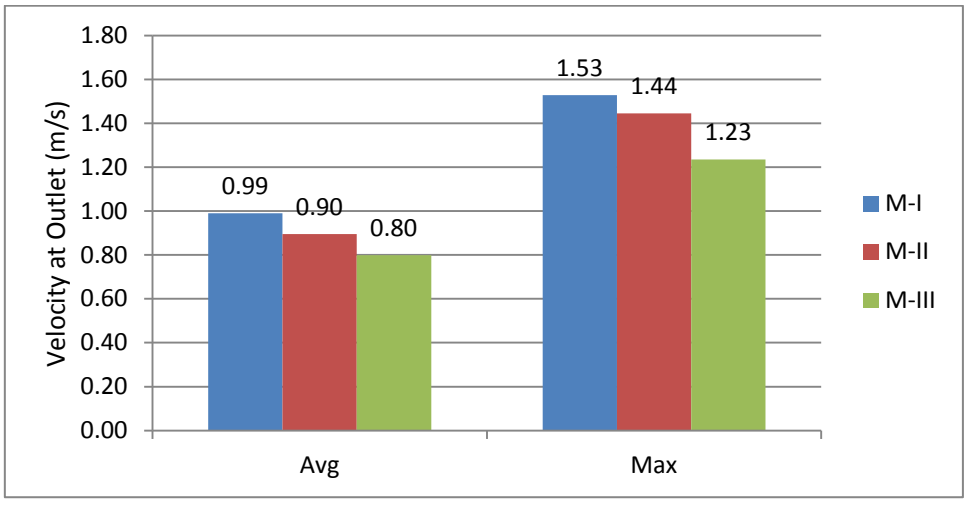


**Figure 39** Showing Velocity at Outlet for M-I M-II & M-III model for Fr = 1.85

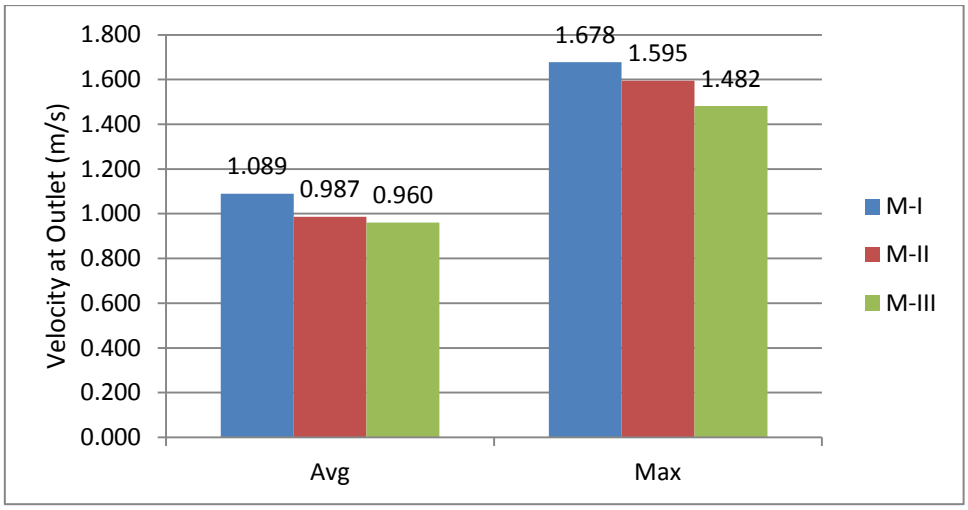


**Figure 40** Showing Velocity at Outlet for M-I M-II & M-III model for Fr = 2.85

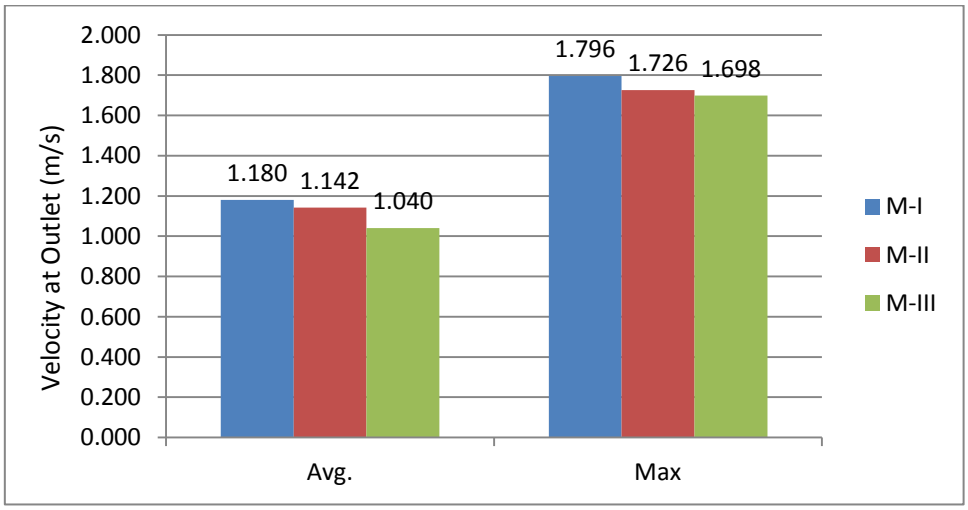


**Figure 41** Showing Velocity at Outlet for M-I M-II & M-III model for Fr = 2.85

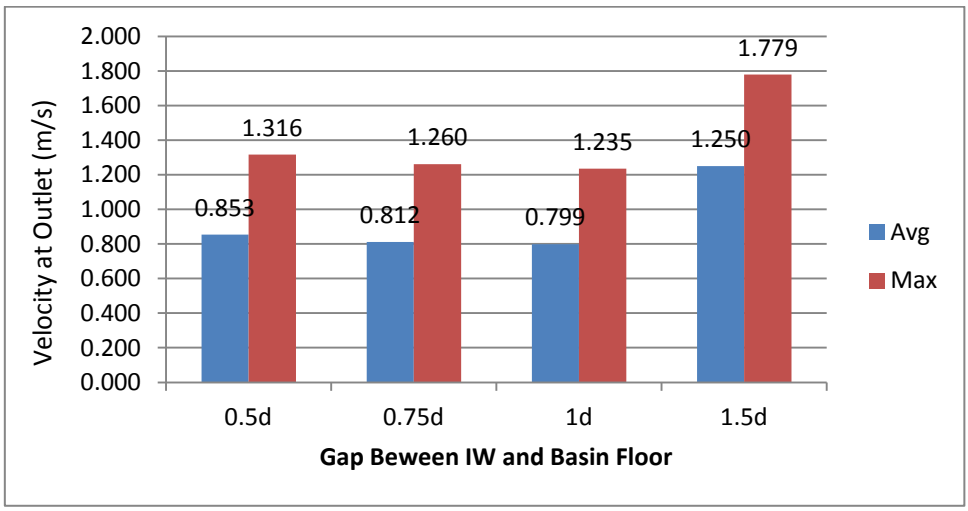


**Figure 42** Velocity at Outlet for M-III M-IV M-V M-VI model for Fr = 1.85

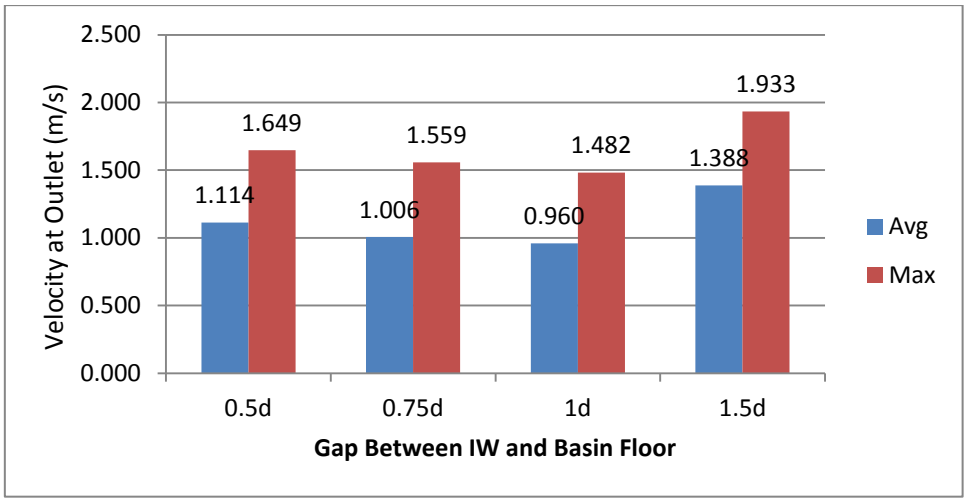


**Figure 43** Velocity at Outlet for M-III M-IV M-V M-VI model for Fr = 2.85

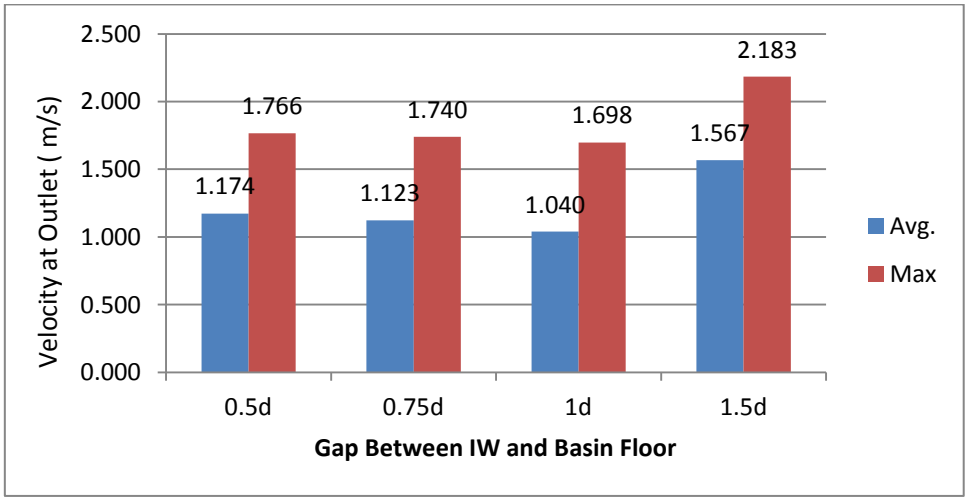


**Figure 44** Velocity at Outlet for M-III M-IV M-V M-VI model for Fr = 3.85

*Shear Stress at Bottom Outlet Plot*

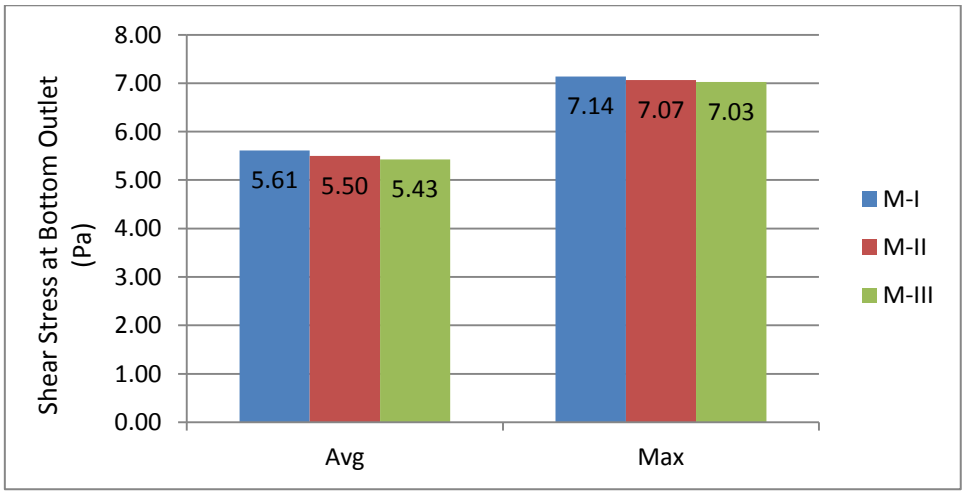


**Figure 45** Showing Shear Stress at Bottom Outlet for M-I M-II & M-III model for Fr = 1.85

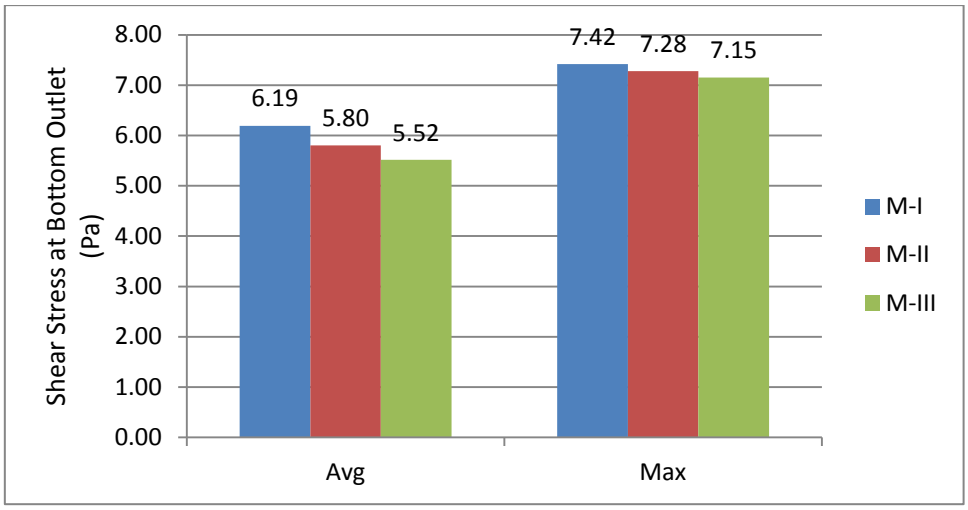


**Figure 46** Showing Shear Stress at Bottom Outlet for M-I M-II & M-III model for Fr = 2.85

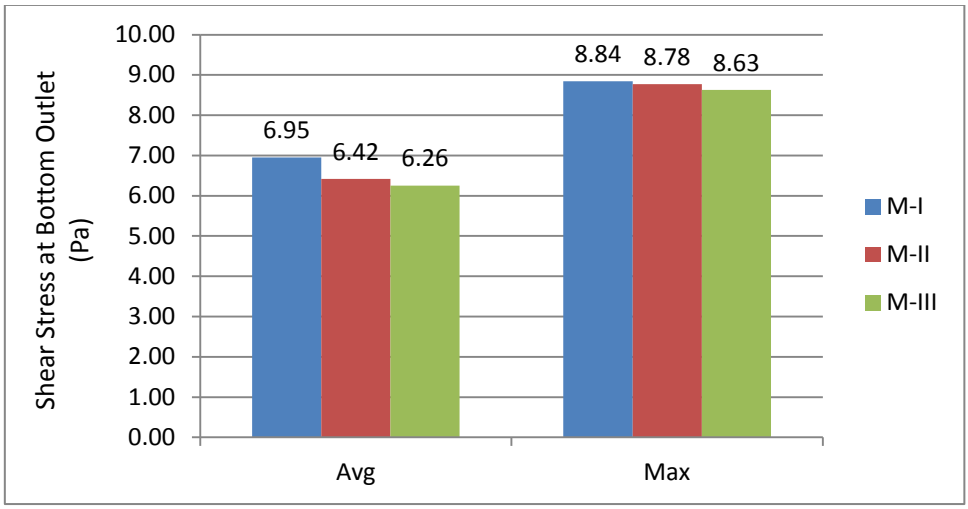


**Figure 47** Showing Shear Stress at Bottom Outlet for M-I M-II & M-III model for Fr = 3.85

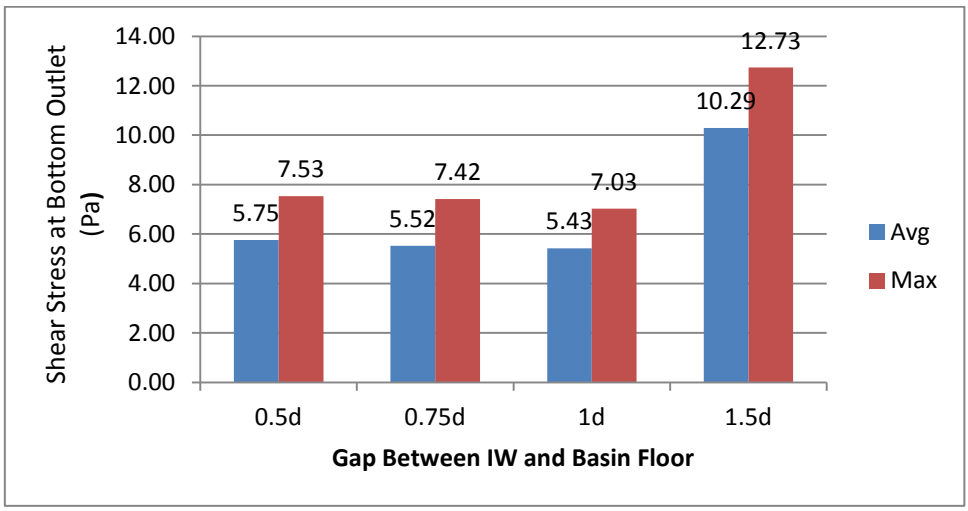


**Figure 48** Shear Stress at Bottom Outlet for M-III M-IV M-V M-VI model for Fr = 1.85

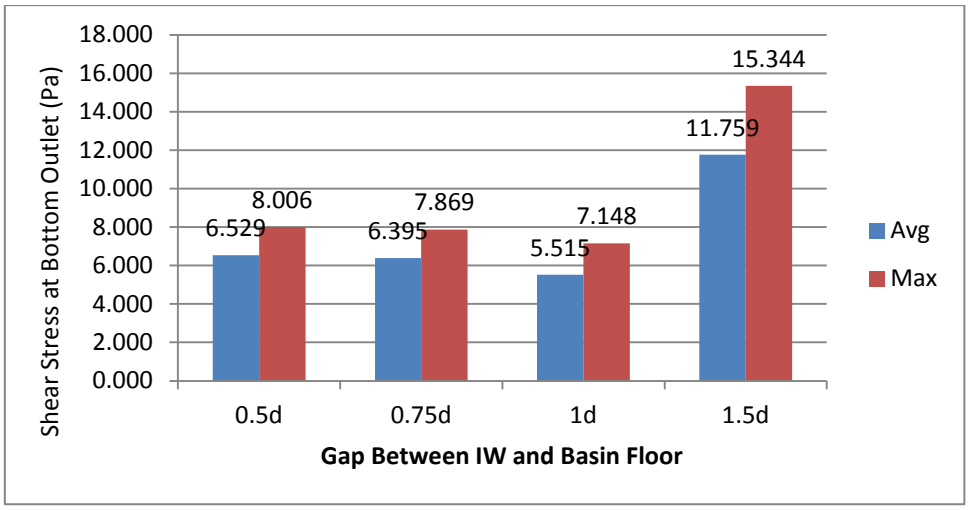


**Figure 49** Shear Stress at Bottom Outlet for M-III M-IV M-V M-VI model for Fr = 2.85

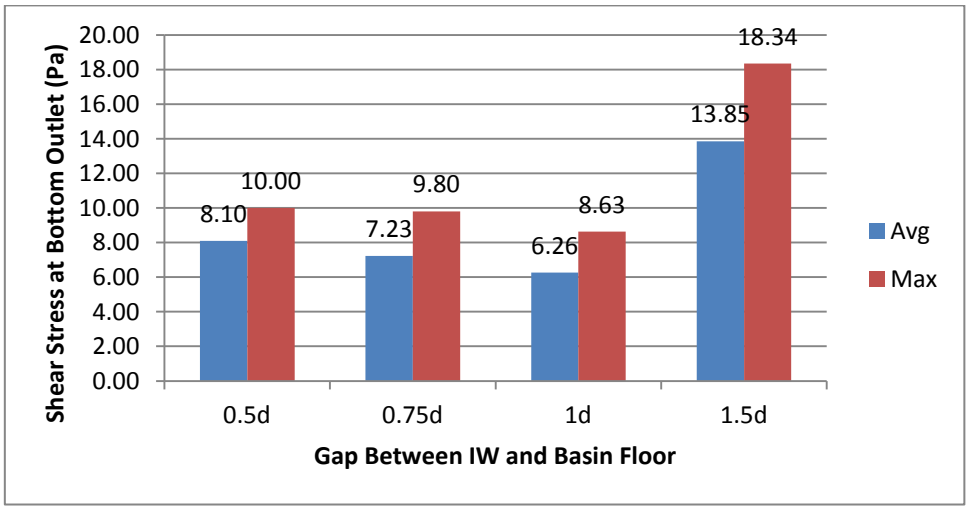


**Figure 50** Shear Stress at Bottom Outlet for M-III M-IV M-V M-VI model for Fr = 3.85

*Energy Losses Plot (Kinetic Energy & Specific Energy Losses)*

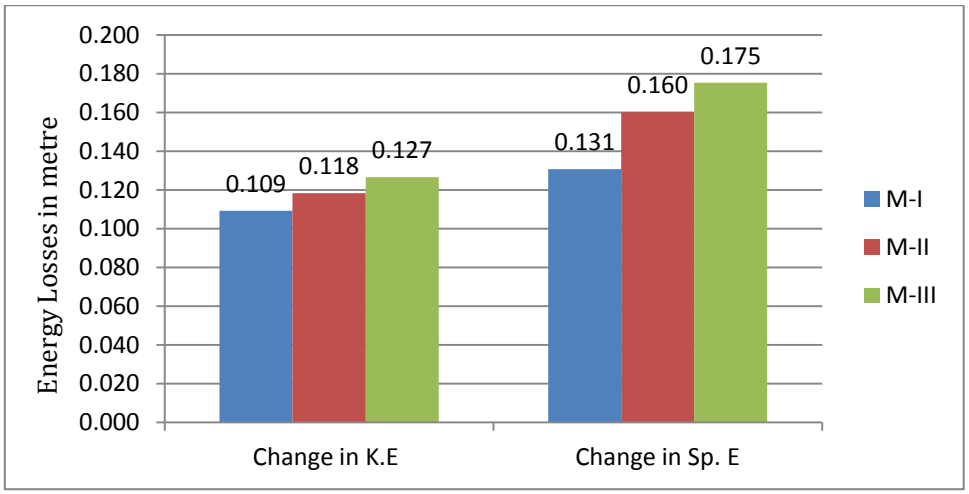


**Figure 51** Showing Energy Losses for M-I M-II & M-III model for Fr = 1.85

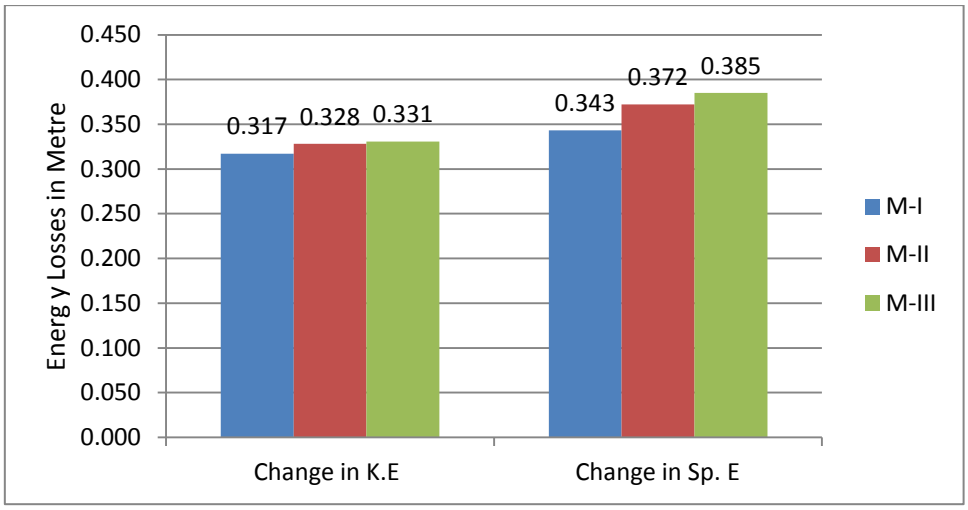


**Figure 52** Showing Energy Losses for M-I M-II & M-III model for Fr = 2.85

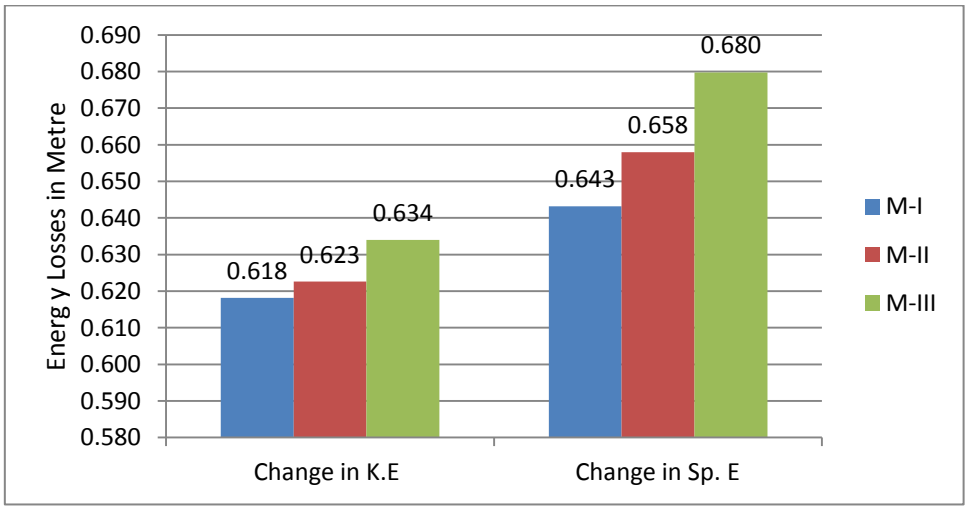


**Figure 53** Showing Energy Losses for M-I M-II & M-III model for Fr = 3.85

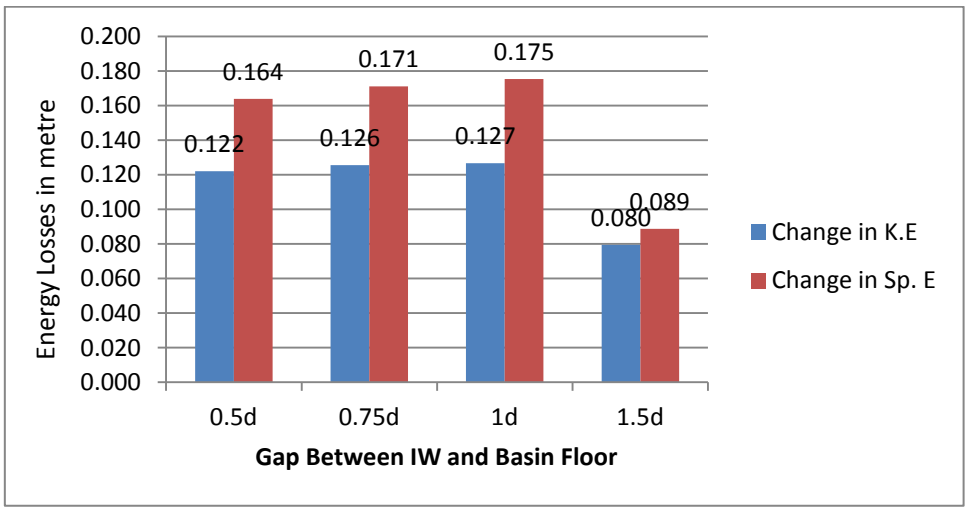


**Figure 54** Energy Losses for M-III M-IV M-V M-VI model for Fr = 1.85

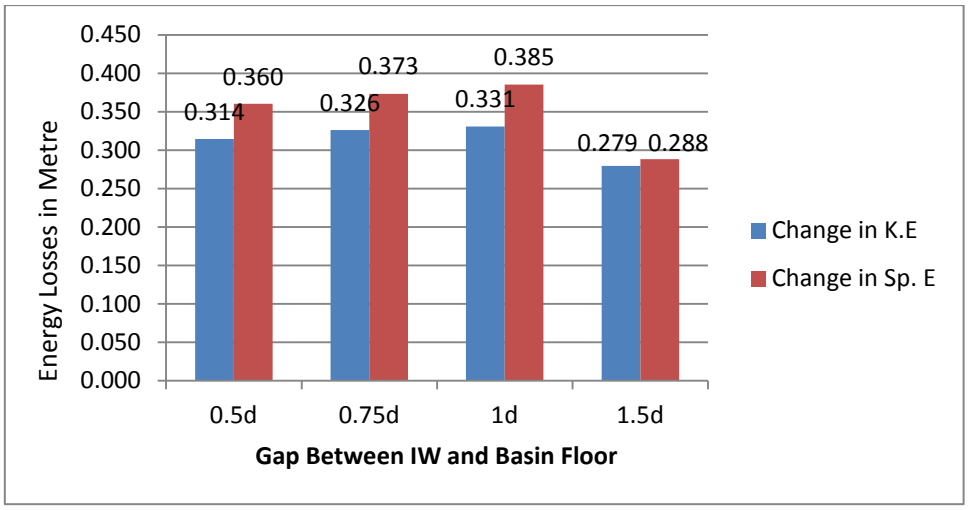


**Figure 55** Energy Losses for M-III M-IV M-V M-VI model for Fr = 2.85

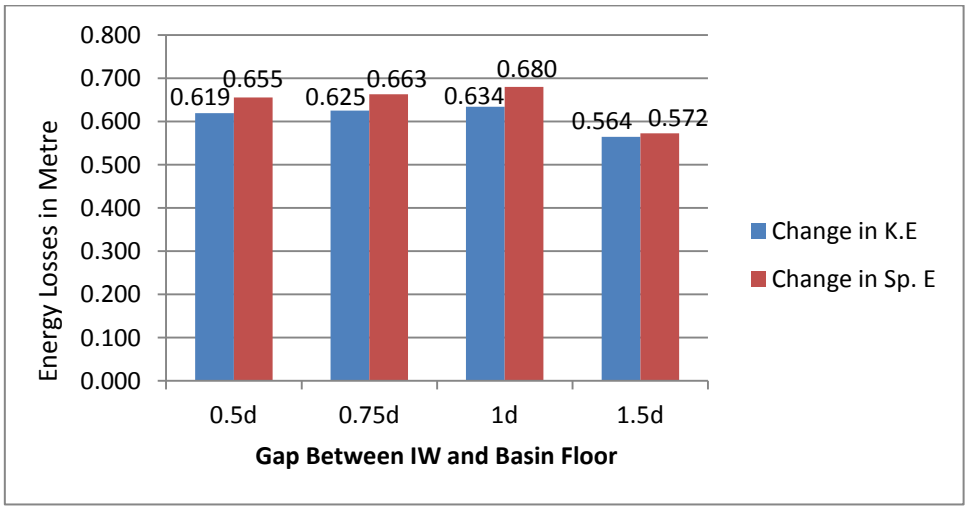


**Figure 56** Energy Losses for M-III M-IV M-V M-VI model for Fr = 3.85

## 5.2 Discussion

For M-I model, the average as well as maximum value of Turbulent Kinetic Energy at the outlet of basin is highest (0.08 for Fr = 1.85, 0.104 for Fr = 2.85 and 0.126 for Fr = 3.85) because the impact wall is so close to the inlet the jet of water strikes with more power causing more turbulence which leads to the formation of horizontal as well as vertical eddies and this can be checked by seeing the stream lines for M-I, M-II and M-III model. For low Froude number (1.85) this effect is more prominent but as the value of Froude number increases (Fr = 3.85) this effect lessens.

For M-III model the value of shear stress at bottom outlet is least (5.43 for Fr = 1.85, 5.52 for Fr = 2.85 and 6.26 for Fr = 3.85) and for M-I model it is highest (5.61 for Fr =1.85, 6.19 for

Fr = 2.85 and 6.95 for Fr =3.85). This is may be because the stream lines of the jet of water are partially hitting the wall causing more portion of jet to pass between the gap hence causing more shearing. This effect is more prominent for high values of Froude number.

The average value of velocity at outlet is least for M-III model (0.80 for Fr =1.85, 0.960 for Fr = 2.85 and 1.040 for Fr =3.85) and highest for M-I model (0.99 for Fr =1.85, 1.089 for Fr = 2.85 and 1.180 for Fr =3.85). This is due to more energy loss in case of M-III than in M-I.

Kinetic energy as well as Specific energy loss is highest in case of M-III model (0.127 for Fr =1.85, 0.331 for Fr = 2.85 and 0.634 for Fr =3.85) and lowest in case of M-I model (0.109 for Fr =1.85, 0.317 for Fr =2.85 and 0.618 for Fr =3.85). This may be because of the of the shearing effect more energy is lost and also may be because the eddies formation at the outlet is least in case of M-III model.

For M-V model the gap between the impact wall and basin floor is least (i.e. 0.5d) hence the shearing area is least which causes value of Turbulent Kinetic Energy, Average Velocity, Shear stress at outlet bottom to be more than other models (M-III, M-IV and M-VI ). But the value of above three parameters is least for M-III model and not M-VI model. This may be because as gap between impact wall and basin floor increases beyond 1d the jet of water that flows between this gap gets shear form one side only as the bottom portion of the wall not able to apply shear to the jet floe which can be seen from the stream lines plot.

# CHAPTER 6

# CONCLUSION

## 6.1 Conclusion Based on Turbulent Kinetic Energy

- As the distance of Impact wall from the inlet increases (M-I to M-III) i.e. from 2d to 4d the value of T.K.E at outlet is increased this due to more eddies are formed in case of M-I model (2d distance from inlet) as the jet of water strikes the impact wall with more power . This leads to more scouring in the downstream direction and hence M-III model is a better option.
- As the gap between the Impact wall and basin floor is increases (M-V to M-VI) i.e. from 0.5d to 1.5d the value of Turbulent Kinetic Energy is decreases from 0.5d to 1d after that it starts to increase because as the gap increases the shearing action of bottom portion of Impact wall and basin floor increases but after 1d the shearing action decreases because the bottom portion of Impact wall does not contribute after 1d. This leads to more scouring downstream of end sill hence M-III model (Gap 1d) is a better option.

## 6.2 Conclusion Based on Outlet velocity

- The outlet velocity for M-III model is least in all three cases of Froude number this is may be because as the distance of Impact wall increases streamlines are more stable due to fewer eddies and more shearing action. As the outlet velocity is less chances of formation of scour will be less hence Model III is a better option.
- Among Models M-V, M-IV, M-III & M-VI, gap between impact wall and basin increases from 0.5d to 1.5d respectively M-III has the least velocity at outlet and hence gap 1d is a better option.

## 6.3 Conclusion based on Energy Losses

- Both Kinetic energy and Specific energy losses are maximum for M-III model due to least value of outlet velocity and depth at outlet. This leads to low Kinetic energy and specific energy at the outlet. Low Kinetic energy ensures less scouring which makes it better option among other five models.

## 6.4 Conclusion based on Wall Shear Stress

- As the distance between the Impact wall and inlet is increased the shearing action is increased because the major portion of jet of fluid passed between the gap between Impact wall and basin floor and hence the shear stress at the bottom of the outlet is decreased. So M-III model is a better option than other models.

Finally it can be concluded that by Simulating different models of Impact Stilling Basin using **ANSYS FLUENT** software **Model M-III** (Impact wall Size 1.5d x 3d, distance between inlet and Impact wall = 4d and a gap of 1d between the basin floor and the wall) is the best option which will produce less Turbulent Kinetic Energy, less outlet velocity, less shear stress at bottom outlet and more Energy losses which will lead to less chances of scouring in the downstream of the end sill. This validates the results obtained by H.L Tiwari and A. Goel.

## 6.5 Future Scope of Study

This study was based on a model and not on an actual prototype whose dimensions are modified by applying suitable model laws. Because of the advancement in technology and presence of CFD software's such as Ansys Fluent analysis can now be done on actual prototype of Impact stilling basin. Also while modelling in fluent certain appurtenances can be added in the geometry like baffle blocks, splitter blocks etc which enhances the energy dissipation process.

# REFERENCES


1. Goel, A. and Verma, D. V. S. (2006), "Development of efficient stilling basins for pipe outlets." ASCE Journal of Irrigation and Drainage Engineering, Vol. 13, No. 4, p. 194-200.

2. Tiwari H. L & Goel A, "Effect of Impact wall on Energy Dissipation in Stilling Basin.", *KSCE Journal of Civil Engineering* (2016) 20(1):463-467.

3. Tiwari H. L. March (2013), "Design of Stilling Basin Model with Impact Wall and end Sill." *Research Journal of Recent Sciences*, Vol. 2(3), 59-63.

4. Tiwari H. L, '*Analysis of Baffle Wall Gap on the Design of Stilling Basin Model*', International Journal of Civil Engineering and Technology, Volume 4, Issue 4, July-August (2013), pp. 66-71.

5. Thomson P.L. and Kilgore R.T., "Hydraulic Design of Energy Dissipators for Culverts and Channels" *Hydraulic Engineering Circular No. 14 (HEC-14)*, Third Edition, Publication No. FHWA-NHI-06-086, July 2006.

6. Tiwari H. L & Goel A, "*Effect of End Sill in the Performance of Stilling Basin Models*", American Journal of Civil Engineering and Architecture, 2014, Vol. 2, No. 2, 60-63.

7. Bradley, J. N. and Peterka, A. J. (1957). "Hydraulic design of stilling basins." Journal of A.S.C.E., Hydraulic Engineering. Vol. 83, No. 5, pp. 1401-1406.

8. Mommandi A. et al.; (2004); Drainage Design Manual, Colorado Department of Transportation (CDOT).